Electronic Supplementary Material (ESI) for ChemComm.

Supporting Information

Supramolecular chirogenesis in zinc porphyrins by enantiopure hemicucurbit[*n*]urils (*n* = 6, 8)

Lukaš Ustrnul,[a] Sandra Kaabel,[a] Tatsiana Burankova,[b] Jevgenija Martõnova,[a] Jasper Adamson,[c] Nele Konrad,[a] Peeter Burk,[d] Victor Borovkov,[a,e] and Riina Aav [a]*

---

* *riina.aav@taltech.ee*

Contents

List of abbreviations

ZnOEP – zinc octaethylporphyrin

ZnTPP – zinc tetraphenylporphyrin

ZnP – zinc porphyrin, therefore in this work ZnOEP or ZnTPP

cycHC[8] – cyclohexanohemicucurbit[8]uril,

cycHC[6] – cyclohexanohemicucurbit[6]uril

cycHC – general abbreviation for both used cyclohexanohemicucurbiturils

NMR –nuclear magnetic resonance spectroscopy

UV-VIS – ultraviolet-visible spectroscopy

CD – circular dichroism

ITC – isothermal titration calorimetry

M1 – (*R*,*R*)-dimethyl-cyclohexa-1,2-diylurea

M2 – (*R*,*R*)-diphenyl-cyclohexa-1,2-diylurea

DCM – dichloromethane

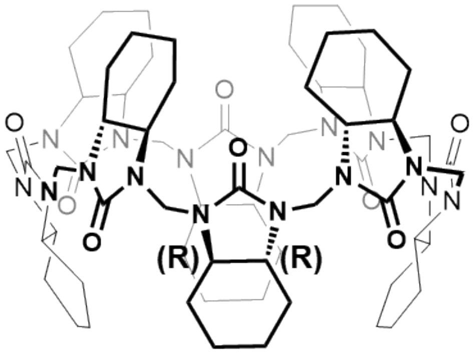

(*R*,*R*)-cycHC[8]

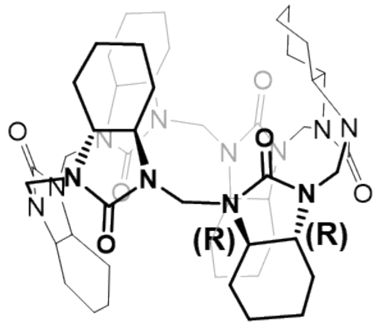

(*R*,*R*)-cycHC[6]

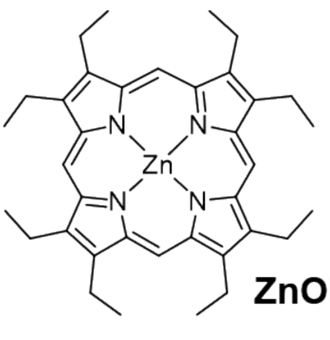

ZnOEP

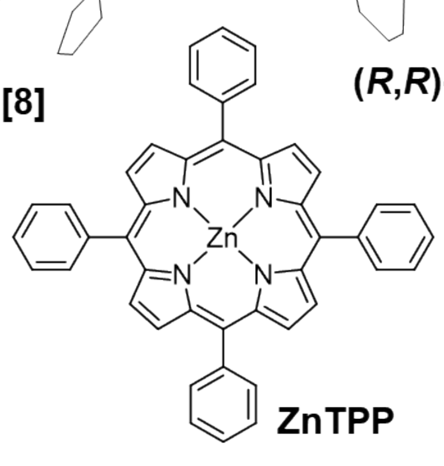

ZnTPP

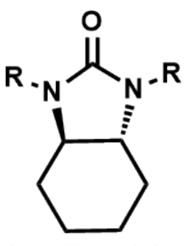

M1 R = Me
M2 R = Ph

1. General information for experimental binding studies

Specification of compounds

Unless otherwise stated, all reagents and solvents was purchased from commercial suppliers and used as received. Compounds prepared in our laboratories was ZnOEP,[1,2] (*S,S*) and (*R,R*) cycHC[8],[3] (*S,S*) and (*R,R*) cycHC[6],[4] (*R*,*R*)-*N*,*N′*-dimethyl-cyclohexa-1,2-diylurea (M1)[5,6] and (*R*,*R*)-*N*,*N′*-diphenyl-cyclohexa-1,2-diylurea (M2). In all cases, except monourea M2, was used procedures as described in literature. Synthesis of new compound monourea M2 was based on the procedure for cyclic ureas published by Lee et al.[7] Toluene for synthesis was dryed over NaH and distilled in advance and stored with molecular sieves under argon atmosphere.

Preparation of samples

All the solutions were prepared using Hamilton® Gastight syringes, those syringes was also used for all the additions during UV-VIS and NMR titrations. For the precise measurement of higher volumes (over 1 ml) was used the mass of solvent and its density instead of volumetric glassware. Samples were weighed on a microbalance with an accuracy of 6 µg (Radwag® MYA 11.4Y, Poland).

NMR measurements

All the ^{1}H NMR experiments was measured on Bruker Avance III 400MHz spectrometer or Bruker Avance III 800MHz spectrometer at temperature 298 K. All NMR titrations and Job plot experiment was carried out in non-deuterated DCM containing 5% of $CDCl_3$ to lock and as a standard. Chemical shifts in ^{1}H NMR were referenced to $CDCl_3$ residual peak at 7.26 ppm and 77.16 ppm at ^{13}C NMR. In all ^{1}H NMR titrations was kept constant concentration of one of the components, usually of porphyrin. The data was analyzed using the program MNova (Mestrelab).

Spectroscopic measurements (UV-VIS, CD)

The UV-VIS absorption spectra were recorded with a Jasco V-730UV-Visible spectrophotometer or with Varian Cary® 50 UV-Vis spectrophotometer. The CD spectra were recorded with a Jasco J-1500 Circular dichroism spectrophotometer. All spectroscopic measurements was done in the DCM.

All the titration experiments were performed in 1 cm screw cap quartz cuvette with septa. The concentration of porphyrins was held constant throughout the titration sequence. The stock solution was kept in the vial with septa and all additions to the cuvette were realized by Hamilton® Gastight syringes to avoid concentration changes caused by the evaporation.

CD measurements were performed in 1 cm screw cap quartz cuvette with septa or in 0.1 cm cuvette with tight cap. The size of cuvette was chosen according to the used concentration of porphyrin. For every sample were accumulated several scans. On all the raw data was used smoothening procedure.

ITC measurements

Calorimetric measurements were performed on a MicroCal PEAQ-ITC calorimeter (Malvern, GE Healthcare Life Sciences). The volume of the calorimetric cell was 200 µl and the size of the syringe was 40 µl. All experiments were carried out in DCM. Due to the limited solubility of porphyrins was cycHC[8] injected by syringe to the ZnTPP solution in the cell. The first smaller addition (0.4 µl), that was used to compensate for diffusion of guest from the injector during equilibration was discarded prior to fitting procedure. The titration was done with additions 0.8 µl having the spacing 80 s.

The heat of dilution was obtained by injecting cycHC[8] to DCM. Prior to data analysis the heat of dilution was subtracted from the corresponding total heat of the interaction. All measurements were carried out at 293 K.

MicroCal PEAQ-ITC analysis software (Malvern) was used for data analysis. Data were fitted using sequential binding model, as initial values for fitting were used association constants obtained from UV-Vis and NMR.

Other instrumentation

Infrared spectra were obtained on a Bruker Tensor 27 FT-IR spectrometer and are reported in wavenumbers. Intensities of the peaks are reported using the following abbreviations: s- strong, m- medium, w-weak. Optical rotation was measured with an Anton Paar MCP 500 polarimeter. Mass spectrometry was measured by direct injection using Agilent G6125B LC/MSD system with APCI-ESI ionization and OpenLAB CDS ChemStation Edition.

2. Circular dichroism measurements

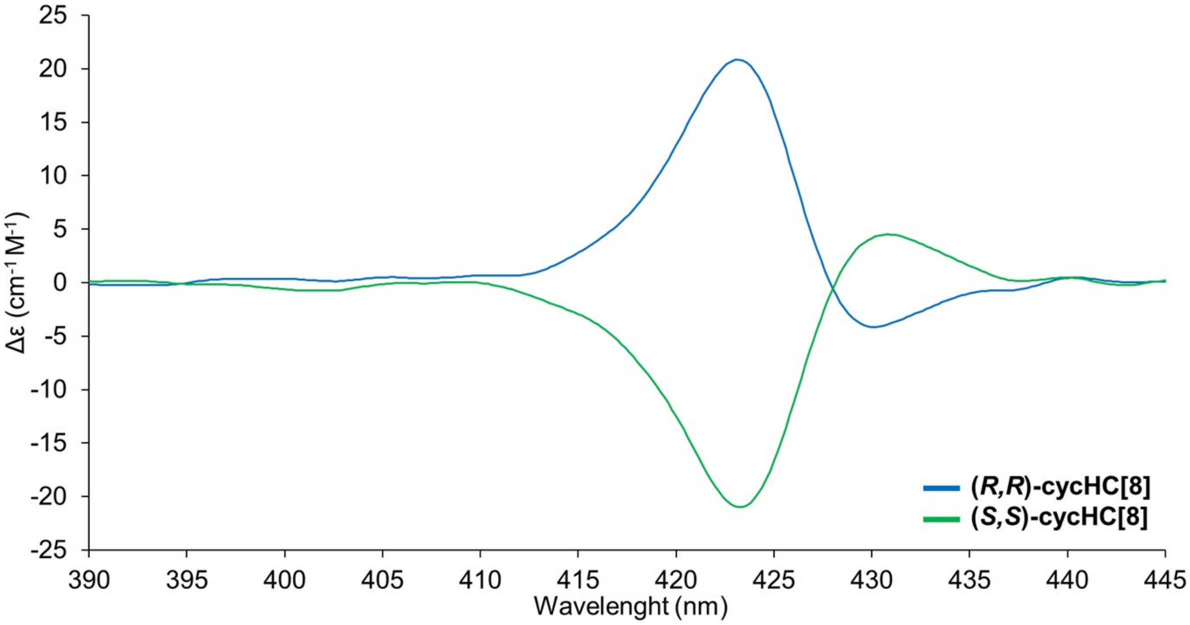

Figure S1. CD of 0.016 mM **ZnTPP** interacting with **cycHC[8]** derivatives (510 eq). More than 90 % of **ZnTPP** is complexed at the selected ratio between the **ZnTPP** and **cycHC[8]**. Solvent: DCM.

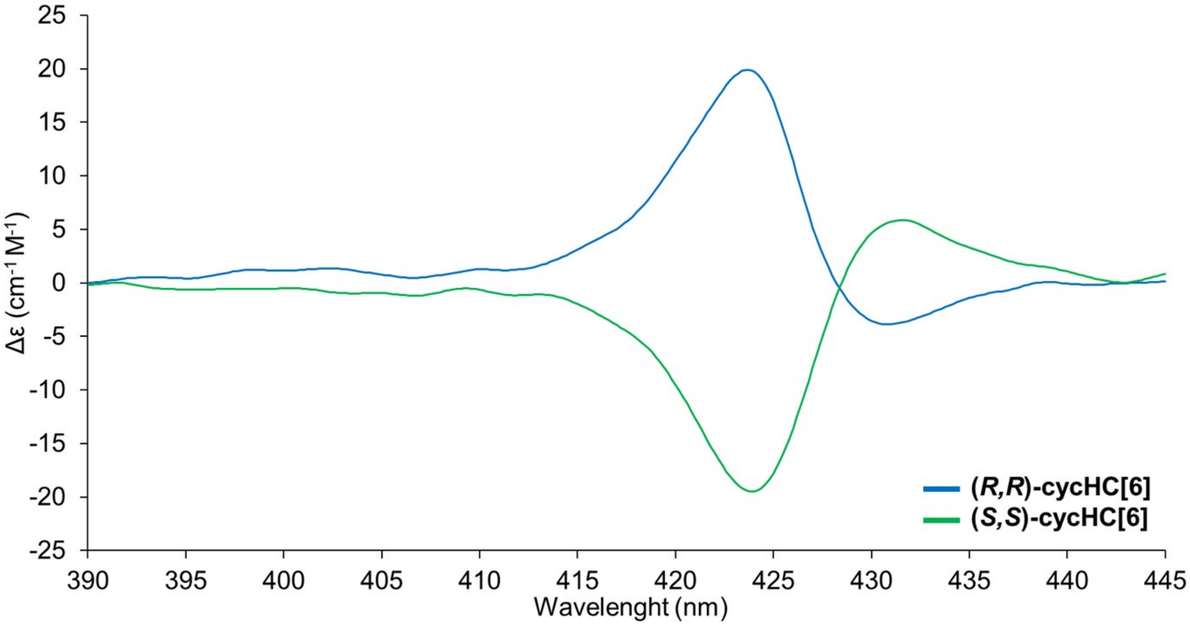

Figure S2. CD of 0.016 mM **ZnTPP** interacting with **cycHC[6]** derivatives (370 eq). More than 90 % of **ZnTPP** is complexed at the selected ratio between the **ZnTPP** and **cycHC[6]**. Solvent: DCM.

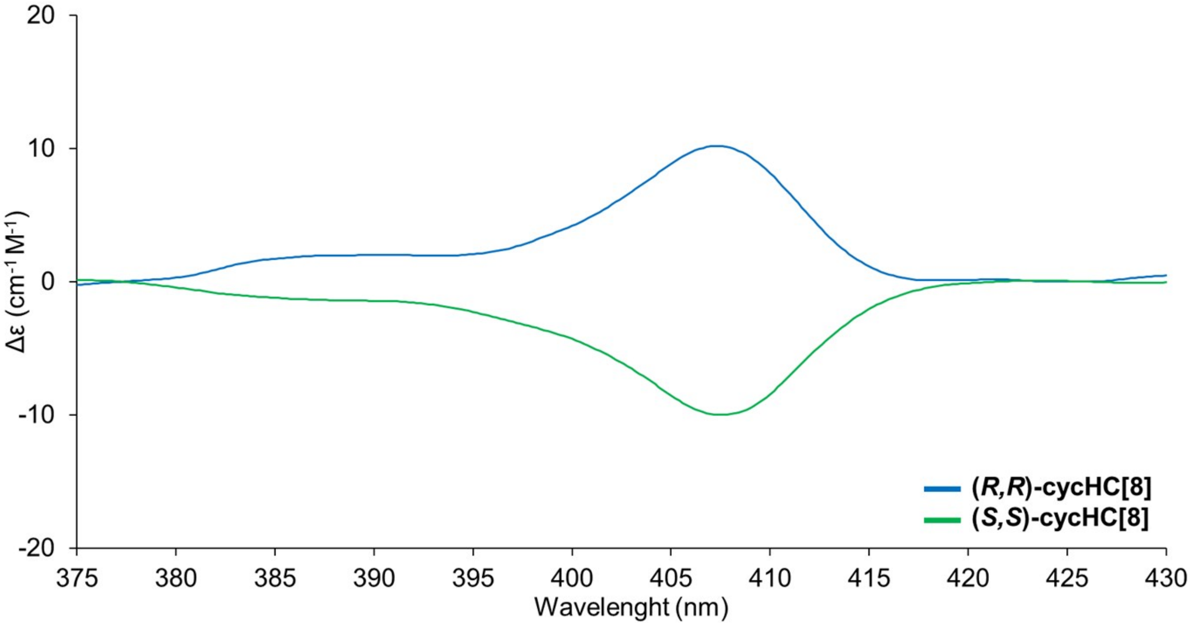

Figure S3. CD of 0.012 mM **ZnOEP** interacting with **cycHC[8]** derivatives (2260 eq). More than 90 % of **ZnOEP** is complexed at the selected ratio between the **ZnOEP** and **cycHC[8]**. Solvent: DCM.

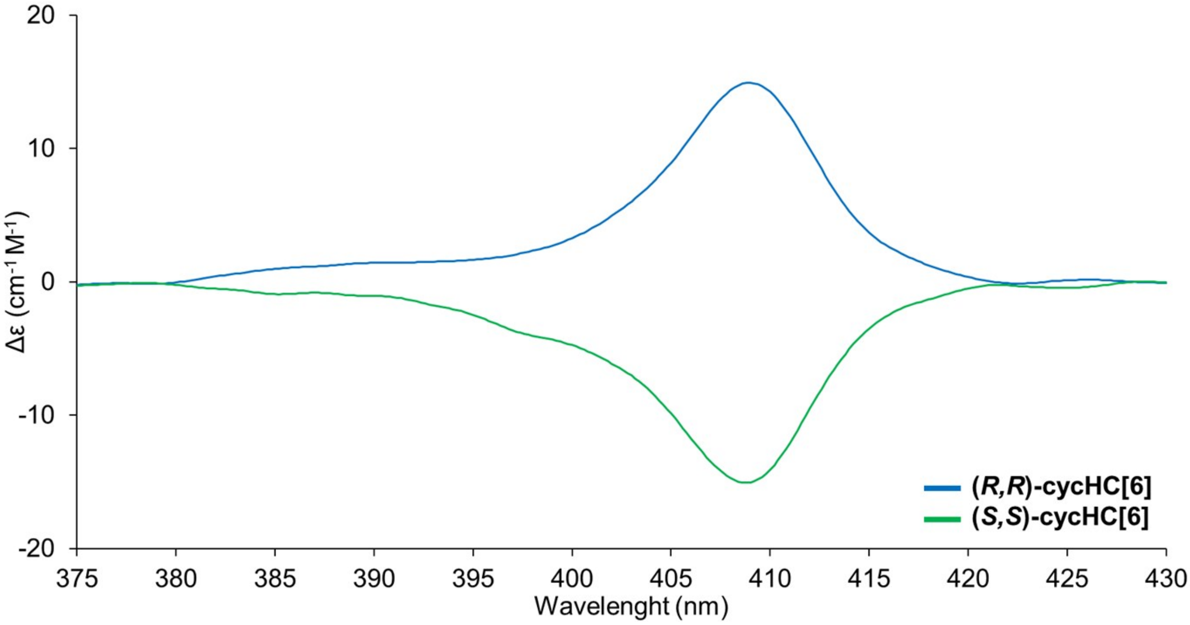

Figure S4. CD of 0.012 mM **ZnOEP** interacting with **cycHC[6]** derivative (1130 eq). More than 90 % of **ZnOEP** is complexed at the selected ratio between the **ZnOEP** and **cycHC[6]**. Solvent: DCM.

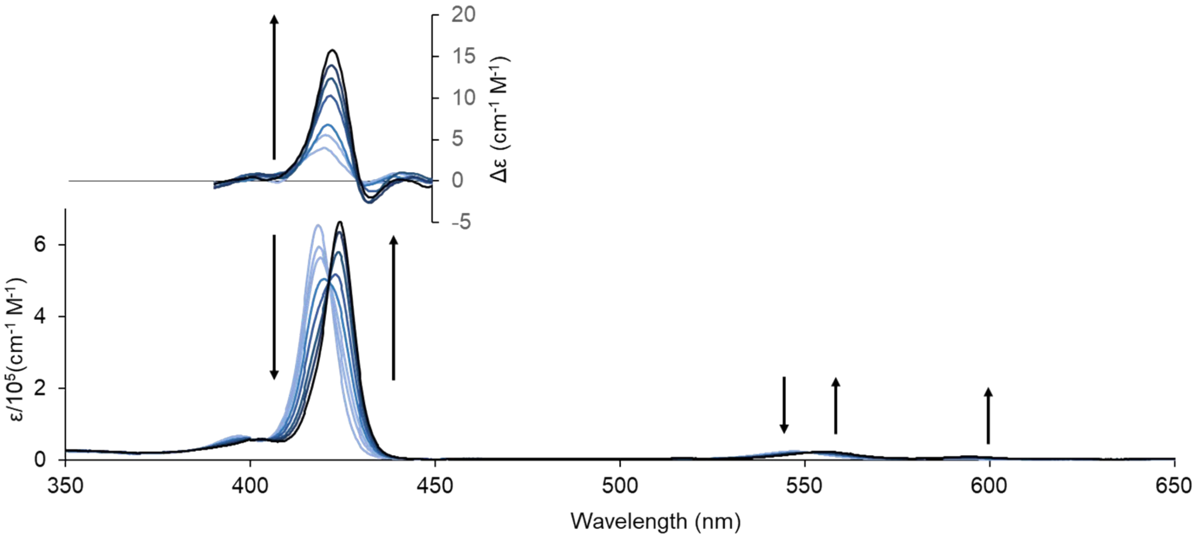

Figure S5. UV-VIS and CD of **ZnTPP** solution (12 µM, DCM) with increasing amount of (*R,R*)-**cycHC[8]** from 5 to 317 equivalents (5, 10, 21, 40, 80, 144, 317 eq.). Experiment is showing direct correlation between concentration of complex and growing induced CD signal.

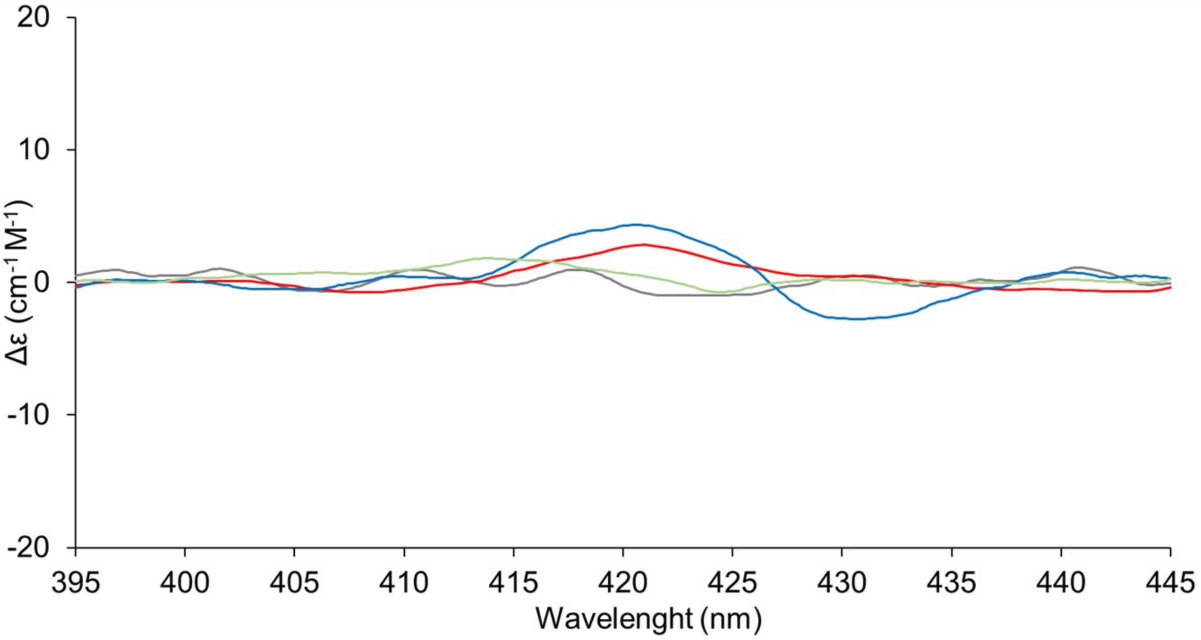

Figure S6. Comparison of CD spectra in DCM for systems without CD signal. CD of 0.012 mM free **ZnTPP** (red) and its complex with 6830 eq of **M1** (blue) (80 % of **ZnTPP** is complexed). CD of 0.016 mM **ZnTPP** and its complex with 6028 eq of **M2** (green) (only 27 % of **ZnTPP** is complexed due to low K_a). Signal for pure dichloromethane (grey) was converted from units of mdeg to $\Delta\varepsilon$($cm^{-1}M^{-1}$) according to **ZnTPP** concentration (0.012 mM) to get same ratio of intensities as in original data.

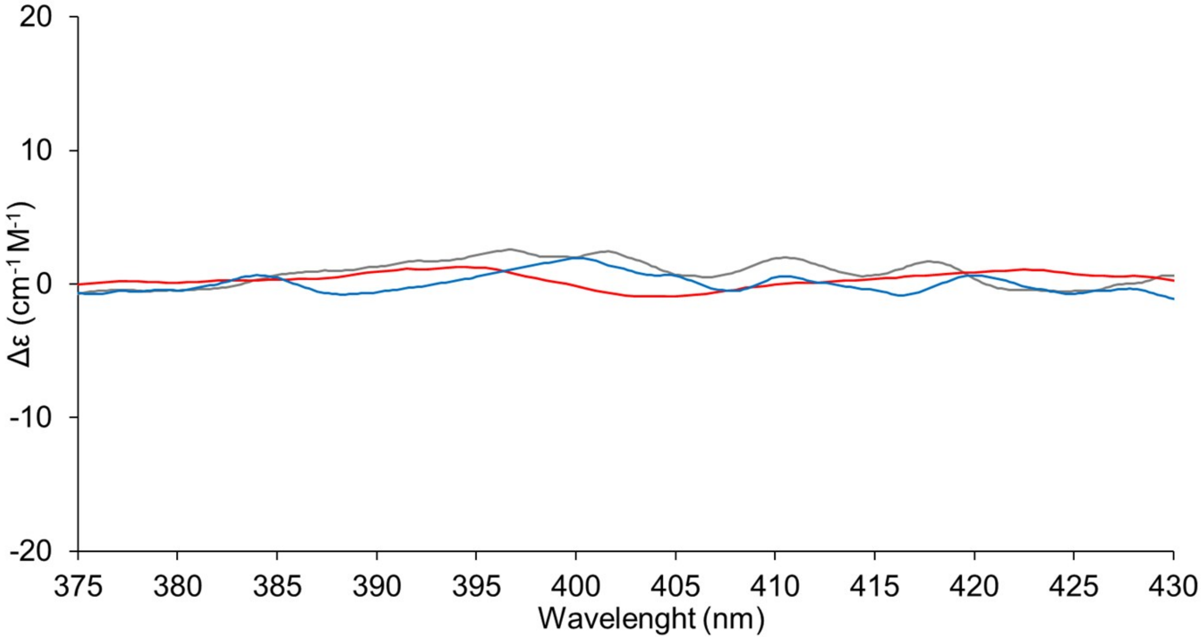

Figure S7. Comparison of CD spectra in DCM for systems without CD signal. CD of 0.012 mM free **ZnOEP** (red) and its complex with 6850 eq of **M1** (blue). Signal for pure dichloromethane (grey) was converted from units of mdeg to Δε($cm^{-1}M^{-1}$) according to **ZnOEP** concentration to get same ratio of intensities as in original data.

3. Computational studies

General information

All calculations were performed using the Gaussian 16 program package.[8] The geometries of complexes between **ZnTPP** and **cycHC[6]** and corresponding reagents were fully optimized using the 1996 correlation and exchange functionals of Perdew, Burke and Ernzerhof[9,10] and newer versions of Ahlrichs split-valence basis sets (def2-SVP).[11,12] Harmonic frequency analysis was used to confirm that the found structures correspond to minima (number of imaginary frequencies equals zero). UV and CD spectra were calculated using TD-DFT approach with Handy and coworkers long-range-corrected version of B3LYP using the Coulomb-attenuating method, CAM-B3LYP,[13] functional and the same def2-SVP basis set.

Modelled UV-VIS and ECD spectra of ZnTPP·(*S,S*)-cycHC[6] complex

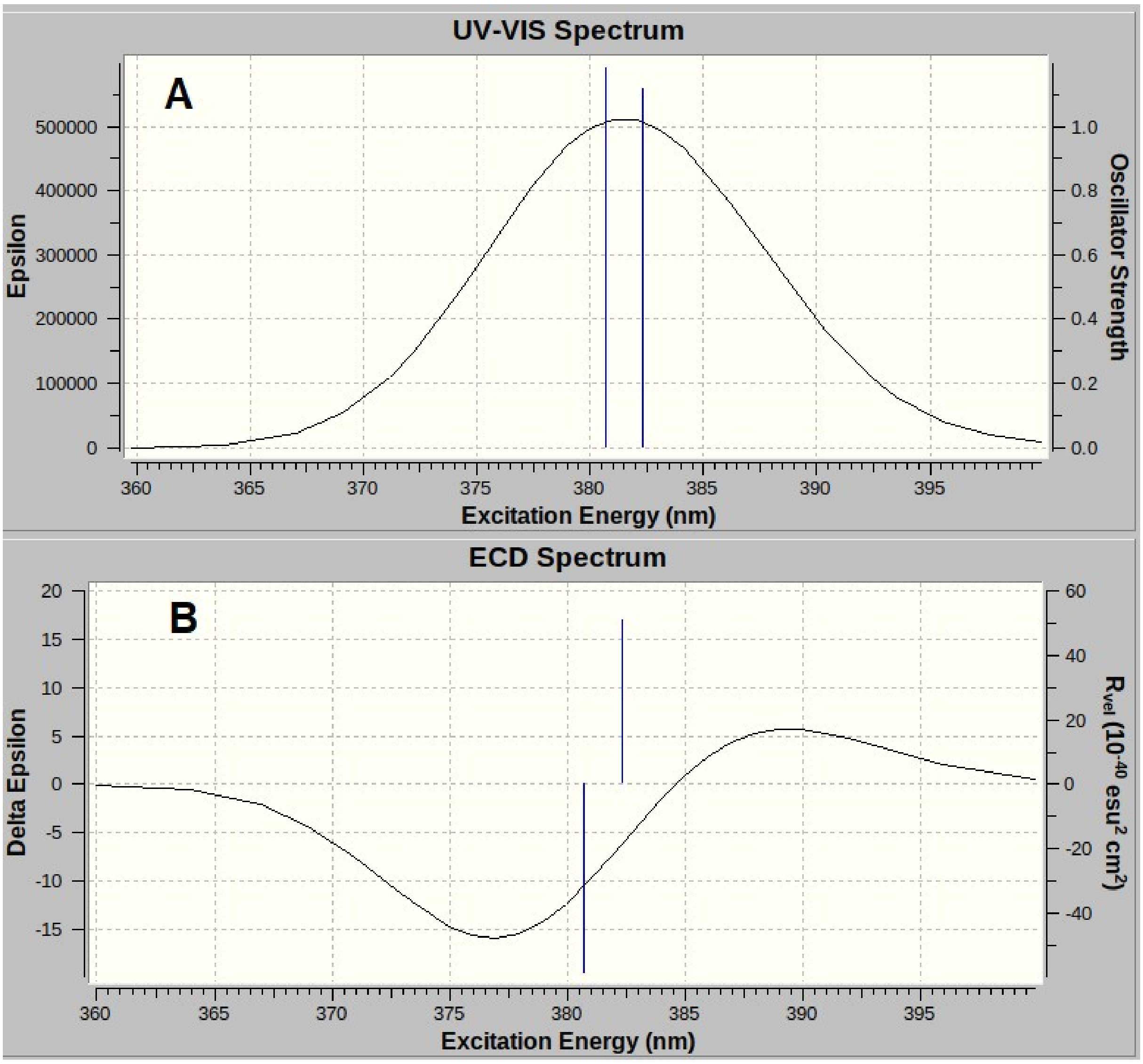

Figure S8. Modelled A) UV-VIS and B) ECD spectra of **ZnTPP**·(*S,S*)-**cycHC[6]** complex. Blue lines correspond to the calculated excitations, oscillator strengths, and rotatory strengths, black line corresponds to the simulated spectrum with peak half-with of 0.06 eV at the half height.

Modelled electronic spectra contained two intense absorption peaks (See Figure S8A, the computed peaks were at least 40 nm shifted to the lower wavelength compared to experimental ones).

Both of above-mentioned strong peaks corresponded to the combined excitations of four following transitions: HOMO→LUMO; HOMO→LUMO+1; HOMO-1→LUMO and HOMO-1→LUMO+1 (see Figures below). The calculated ECD spectrum also had the strongest values corresponding to those two high-absorption peaks, but with opposite signs (see Figure S8B).

Molecular orbitals involved in UV-VIS and circular dichroism transitions

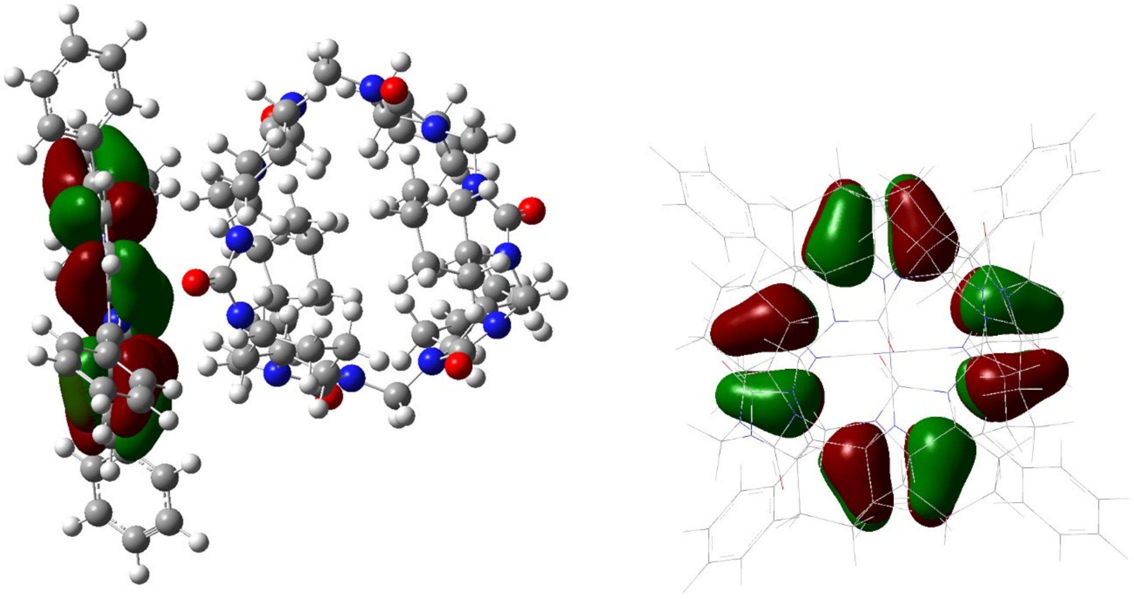

Figure S9. Computational model of orbital HOMO-1

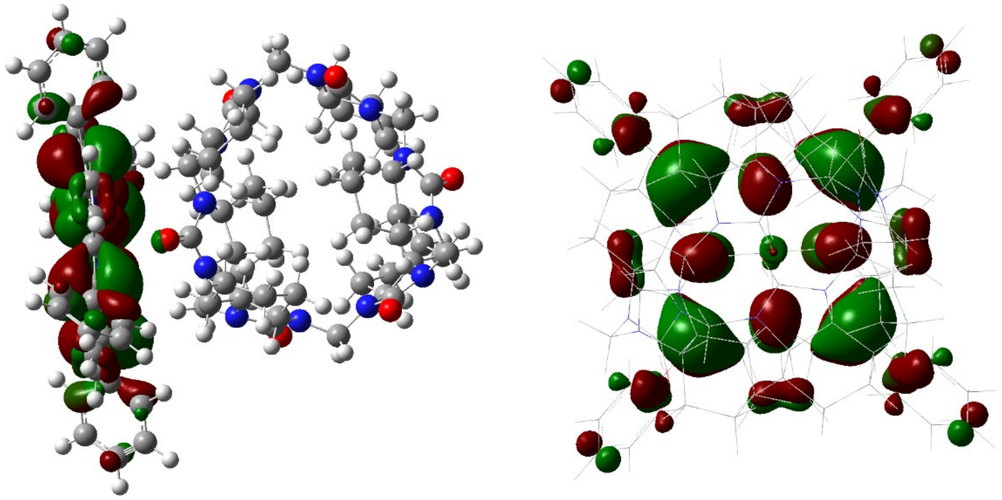

Figure S10. Computational model of orbital HOMO

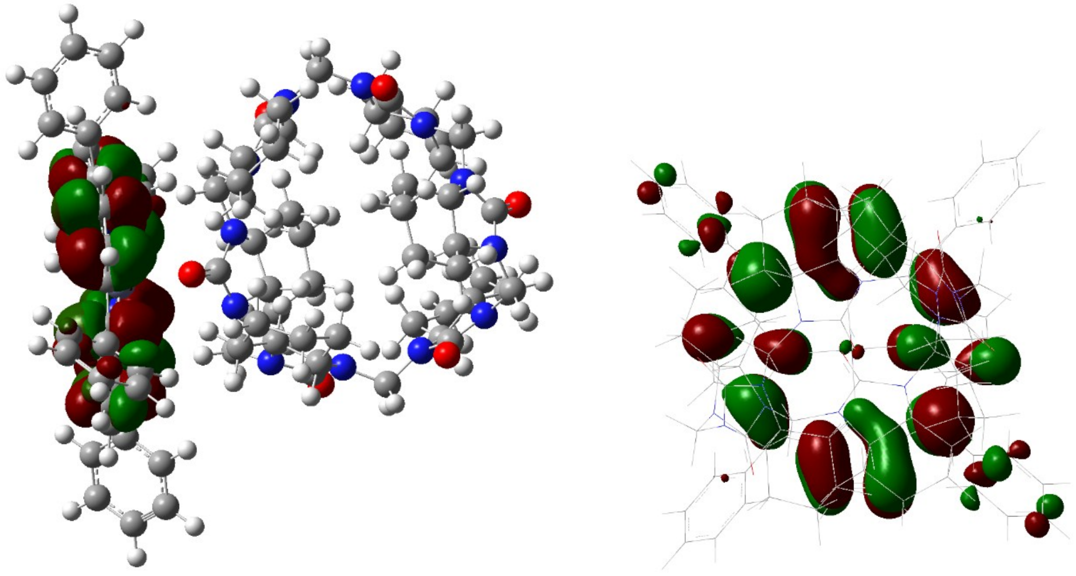

Figure S11. Computational model of orbital LUMO

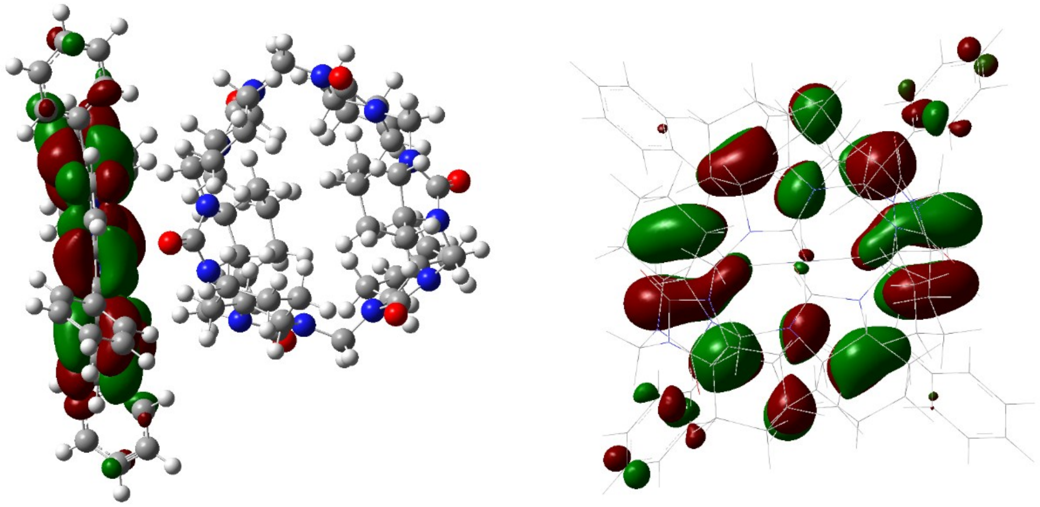

Figure S12. Computational model of orbital LUMO+1

xyz-Coordinates of ZnTPP·cycHC[6] complex

C	-0.111256	-1.052794	2.646504
C	-0.111143	-1.742423	4.005959
C	-1.317126	-1.187603	4.797319
C	-1.391440	0.353848	4.839565
C	-1.269801	1.017375	3.449589
C	0.001955	0.464948	2.820116
N	0.962452	-1.310909	1.681597
C	1.183546	-0.162786	0.939420
N	0.447420	0.873560	1.484316
O	1.927131	-0.075364	-0.061370
C	0.622482	2.258127	1.071190
C	-1.648503	3.011882	-3.799161
C	-0.326717	2.270648	-3.507362
C	-0.216700	1.749319	-2.057731
C	-1.994038	4.111704	-2.770340
C	-1.900942	3.480078	-1.385783
C	-0.489828	2.935229	-1.141172
N	-0.492571	2.790474	0.315300
N	-2.104824	4.292371	-0.184543
C	-3.330489	5.026519	0.086854
C	-1.344423	3.755867	0.861150
O	-1.404112	4.081718	2.048156
C	0.216398	-2.040785	-3.370433
C	-1.061847	-2.819738	-3.744721
C	-2.037178	-3.007485	-2.562567
C	0.939898	-2.583192	-2.117213
C	-0.099370	-2.683007	-1.005644
C	-1.234746	-3.624438	-1.423201
N	-1.851420	-3.916416	-0.130979
N	0.257119	-3.227703	0.305849
C	1.274269	-2.636163	1.157316
C	-0.875315	-3.840093	0.864625
O	-0.986338	-4.245903	2.022204
C	-5.154321	-3.056017	3.833400
C	-6.472215	-2.341363	3.466487
C	-7.148319	-2.883445	2.187095
C	-4.156405	-3.151665	2.658837
C	-4.908389	-3.782534	1.493096
C	-6.091897	-2.897262	1.087809
N	-6.406373	-3.431226	-0.238334
N	-4.263775	-3.999725	0.199509
C	-3.031898	-4.745150	0.027610
C	-5.238833	-3.962586	-0.801378
O	-5.097028	-4.339203	-1.965864
C	-5.004134	-1.249838	-4.723223
C	-5.015957	0.293630	-4.741965
C	-5.165894	0.927592	-3.341822
C	-6.172861	-1.880209	-3.932982
C	-6.202382	-1.215261	-2.561270
C	-6.398849	0.297911	-2.704114
N	-6.825172	0.655141	-1.352308
N	-7.250402	-1.550593	-1.595980
C	-7.461342	-2.895539	-1.084622
C	-7.496769	-0.432535	-0.788275
O	-8.188865	-0.408295	0.230904
C	-6.140731	2.040082	3.651531

C	-4.874034	2.869300	3.952936
C	-4.605958	4.002697	2.937446
C	-6.214226	1.531440	2.195354
C	-6.031188	2.747305	1.294755
C	-4.660144	3.384870	1.544545
N	-4.512785	4.223070	0.354070
N	-6.022744	2.622991	-0.161456
C	-7.095525	2.014503	-0.924892
C	-5.238971	3.648323	-0.697511
O	-5.202637	3.990513	-1.880400
H	-1.092700	-1.268648	2.152570
H	0.846134	-1.532978	4.530461
H	-0.209482	-2.839554	3.883687
H	-1.303163	-1.590063	5.831255
H	-2.246848	-1.580507	4.330206
H	-2.337833	0.669907	5.326045
H	-0.572431	0.742336	5.485139
H	-2.144738	0.765023	2.810319
H	-1.240131	2.122994	3.529188
H	0.843546	0.668817	3.531452
H	-1.615963	3.448884	-4.818644
H	-2.482645	2.275844	-3.809765
H	0.531021	2.953241	-3.697038
H	-0.201956	1.428622	-4.219645
H	-0.964470	0.948482	-1.863256
H	0.785076	1.312290	-1.871259
H	-1.282158	4.962750	-2.843399
H	-3.017884	4.495137	-2.953552
H	-2.608083	2.611627	-1.362119
H	0.242330	3.738675	-1.414598
H	-0.050191	-0.978059	-3.181613
H	0.915394	-2.025563	-4.231919
H	-1.579665	-2.310021	-4.583970
H	-0.778952	-3.825248	-4.129096
H	-2.455989	-2.030279	-2.234544
H	-2.898540	-3.646163	-2.845454
H	1.379684	-3.586423	-2.309662
H	1.765879	-1.902402	-1.831087
H	-0.542731	-1.663293	-0.865407
H	-0.772144	-4.568576	-1.814371
H	-5.382697	-4.087134	4.184424
H	-4.676292	-2.542647	4.693803
H	-7.180329	-2.399392	4.318906
H	-6.266033	-1.258965	3.315135
H	-7.537737	-3.912641	2.346758
H	-7.996456	-2.229752	1.900737
H	-3.793537	-2.142316	2.363116
H	-3.261546	-3.745200	2.936088
H	-5.317936	-4.763287	1.852435
H	-5.706909	-1.851274	0.976911
H	-4.051970	-1.597728	-4.265952
H	-5.001232	-1.637611	-5.762951
H	-4.091941	0.669520	-5.228964
H	-5.858701	0.645246	-5.378213
H	-5.257400	2.030936	-3.405110
H	-4.273122	0.716043	-2.712474
H	-6.015340	-2.972683	-3.830891
H	-7.142036	-1.713342	-4.451853

H	-5.202394	-1.380656	-2.084697
H	-7.259780	0.470332	-3.402498
H	-6.203531	1.182942	4.354202
H	-7.041394	2.662517	3.851527
H	-3.991558	2.192338	3.954765
H	-4.936196	3.289990	4.977930
H	-3.609379	4.450744	3.123999
H	-5.371765	4.804330	3.022640
H	-7.175472	1.016240	1.994515
H	-5.406625	0.793858	1.991260
H	-6.817179	3.495076	1.580735
H	-3.897306	2.565362	1.509396
H	-2.866306	-5.387878	0.917893
H	-3.153709	-5.381528	-0.874400
H	-3.133201	5.670420	0.965141
H	-3.564036	5.662166	-0.788500
H	-8.015497	1.989416	-0.303456
H	-7.266851	2.649828	-1.819413
H	1.547338	2.309640	0.462370
H	0.748538	2.889564	1.975301
H	1.433071	-3.323180	2.009663
H	2.217601	-2.545467	0.588126
H	-8.404803	-2.876823	-0.506404
H	-7.570412	-3.587927	-1.941064
Zn	4.115456	0.175260	-0.084625
N	4.534172	-0.605867	1.816367
N	4.668335	-1.660454	-0.914003
N	4.290931	1.043198	-1.972532
N	4.140583	2.093976	0.756308
H	3.771489	-7.508228	1.685607
H	5.718194	4.749724	-3.016730
H	2.187229	2.858565	4.317867
H	6.153462	1.310617	5.121658
H	6.036267	2.213822	7.448669
H	3.988206	3.442363	8.222429
H	2.063210	3.762974	6.640889
H	3.392529	-5.209179	0.786350
H	3.148687	-3.001317	-4.514211
H	3.373040	-3.884070	-6.841213
H	5.119184	-2.944462	-8.381578
H	6.637207	-1.118075	-7.566629
H	6.406301	-0.240493	-5.238889
H	6.989791	-3.831982	2.772133
H	7.375775	-6.131934	3.673252
H	5.766519	-7.981921	3.134601
H	5.491659	7.063785	-3.931048
H	3.508255	8.474440	-3.314733
H	1.759695	7.546247	-1.768550
H	1.994317	5.234994	-0.856341
H	4.257122	-0.646944	5.168813
H	4.650590	-3.094919	4.076359
H	5.688174	-4.864978	-0.892460
H	5.530790	-3.785354	-3.373407
H	3.972226	0.993978	-5.319711
H	3.639716	3.450517	-4.228837
H	4.213596	5.456317	0.745188
H	4.319301	4.370686	3.224759
C	4.484336	-6.704084	1.925189

C	4.842728	5.361789	-2.751812
C	3.033514	2.714349	5.007141
C	4.174834	2.010000	4.558685
C	5.250212	1.840257	5.460755
C	5.183506	2.351189	6.765805
C	4.040009	3.042214	7.198196
C	2.964979	3.222897	6.313171
C	4.270548	-5.413042	1.418763
C	3.915117	-2.587488	-5.187008
C	4.043043	-3.082338	-6.493742
C	5.017288	-2.555446	-7.356814
C	5.862730	-1.530788	-6.901625
C	5.732417	-1.033916	-5.596116
C	4.754327	-1.551448	-4.715496
C	5.163090	-4.358622	1.720310
C	6.279365	-4.640193	2.540570
C	6.495308	-5.932296	3.042918
C	5.597858	-6.968684	2.738628
C	4.715123	6.662731	-3.261335
C	3.608447	7.454196	-2.913611
C	2.632618	6.935783	-2.047269
C	2.762662	5.635956	-1.535045
C	3.867047	4.823098	-1.881315
C	4.375329	0.060027	3.011523
C	4.388922	-0.892358	4.109754
C	4.588857	-2.133104	3.556378
C	4.693538	-1.939804	2.119811
C	4.930010	-2.981557	1.183008
C	4.967843	-2.816680	-0.227460
C	5.359804	-3.856162	-1.163878
C	5.279065	-3.309076	-2.420115
C	4.831376	-1.936242	-2.253546
C	4.620715	-1.023747	-3.322213
C	4.325682	0.358270	-3.166237
C	4.043412	1.270114	-4.262466
C	3.873193	2.515293	-3.709074
C	4.050590	2.364892	-2.273845
C	4.005192	3.435477	-1.339173
C	4.102846	3.289292	0.071216
C	4.177670	4.394784	1.011279
C	4.231564	3.844741	2.268234
C	4.197652	2.402342	2.097482
C	4.243138	1.466453	3.165972

4. Binding data analysis.

The titration (NMR and UV-VIS) data were fitted using **numpy** (1.10.2) and **scipy** (0.18.1) libraries of Python 3. The scripts (NMR – globfit_NMR_SI.py, UV-VIS – globfit_UVVIS_SI.py) allow for simultaneous fitting of several datasets, which significantly improves stability of the fit results. This is essential in the case of 1:3 and 1:4 binding calculations. The **leastsq** function (implementation of the Levenberg-Marquadt algorithm) was used to determine the parameter set including the association constants K_1, K_2, and K_3 that minimizes $\chi^2 = \sum [f(x_i) - y_i]^2$, where $f(x_i)$ is the theoretical value of the traced quantity (chemical shift, absorbance) for a given pair of the host and guest concentration $x_i = (c_{host0,i}, c_{guest0,i})$; y_i is the corresponding experimental value. The concentrations of the free host and guest molecules as well as their complexes are calculated numerically (function **scipy.fsolve**), using the definition of the binding constants and the mass balance equations:

$$K_1 = \frac{[cycHC \cdot ZnP]}{[cycHC] \cdot [ZnP]}$$

$$K_2 = \frac{[cycHC \cdot ZnP_2]}{[cycHC \cdot ZnP] \cdot [ZnP]}$$

$$K_3 = \frac{[cycHC \cdot ZnP_3]}{[cycHC \cdot ZnP_2] \cdot [ZnP]}$$

$$[cycHC]_0 = [cycHC] + [cycHC \cdot ZnP] + [cycHC \cdot ZnP_2] + [cycHC \cdot ZnP_3]$$

$$[ZnP]_0 = [ZnP] + [cycHC \cdot ZnP] + 2[cycHC \cdot ZnP_2] + 3[cycHC \cdot ZnP_3]$$

To ensure monotonous change of the calculated concentrations, the system of the equations is first solved for the lowest $[ZnP]_0$, if $[cycHC]_0$ is constant (or for the lowest $[cycHC]_0$, if $[ZnP]_0$ is constant). The obtained values are then passed to scipy.solve as inital guesses for the next pair of $[ZnP]_0$ and $[cycHC]_0$. The procedure continues for all data points in the titration curve.

To stabilize the fit results the following physically reasonable constraints were applied:
1. The chemical shifts of both ZnP and cycHC change monotonously as the number of ZnP molecules in the complex increases.
2. The K_3 value is very sensitive (intertwined) to the values of the chemical shifts for $[cycHC \cdot ZnP_3]$. Therefore, in case the chemical shift exhibited anomalous decrease for the $[cycHC \cdot ZnP_3]$ with concurrent increase of K_3, a more strong constraint then 1 was applied: we assumed a linear dependence of the chemical shifts on the number of guest molecules (see ZnTPP, cycHC[8] – NMR3, CH1 and CH2 signals of cycHC[8]).
3. For the analysis of the UV-Vis spectra we assumed that porphyrin absorption is mainly influenced by the interaction with the host molecule, but significantly less by porphyrins complexed to the same host. Therefore, in the fit model the absorption of the HG complex was considered similar to those of HG_2 and HG_3.

Errorbars of the fit parameters were estimated from the covariance matrix.
Experimental points and fitted values can be found in a file: titration data-complete.xlsx.

The fitting routine converges and stable values of all three association constant are obtained only if extensive amount of experimental data is used. On the other hand, even one titration can provide K_1 values suitable for stability comparison of the particular systems, partly because the mechanism of binding is similar in all cases.

5. Binding studies

UV-VIS titrations

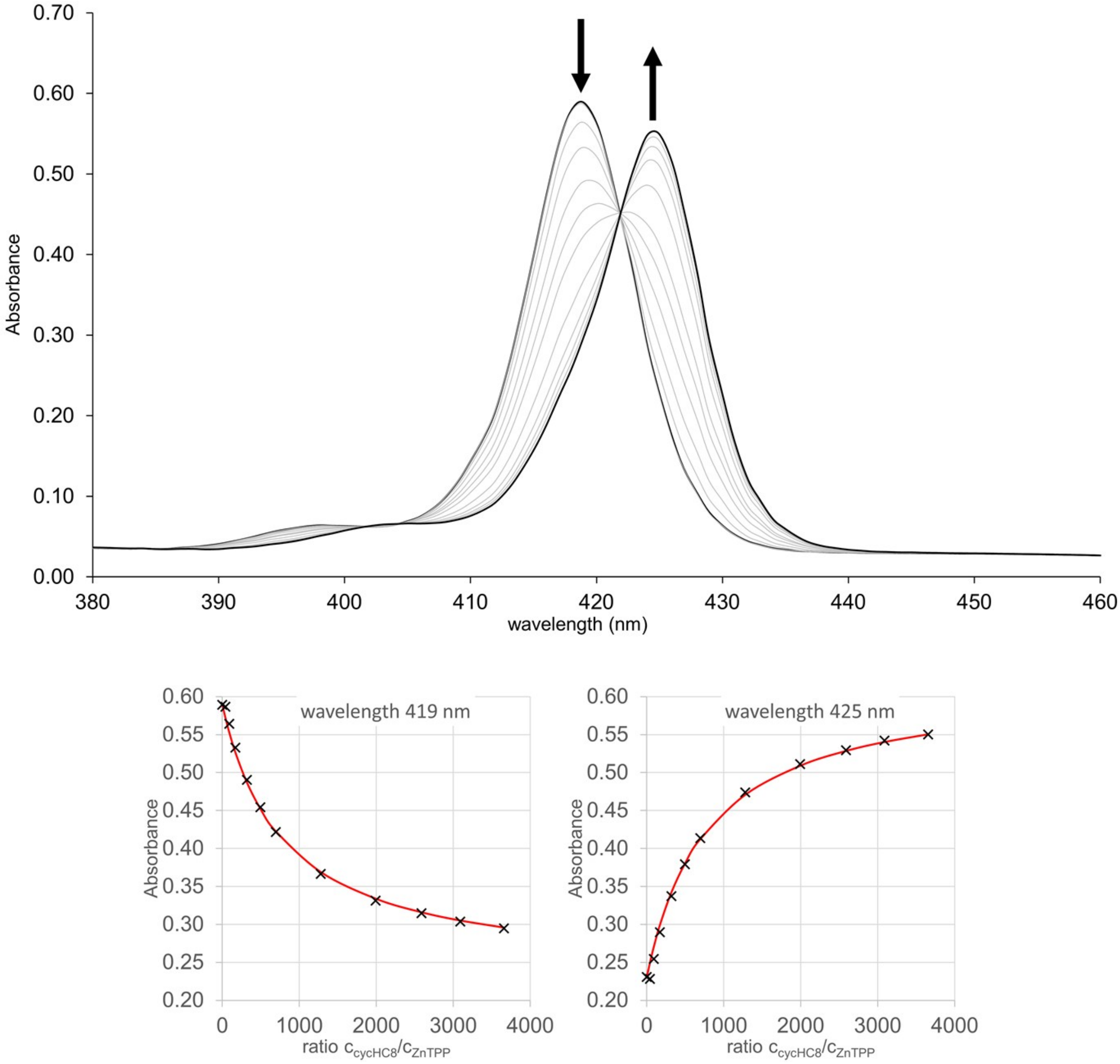

Figure S13. Up: UV-VIS titration of **ZnTPP** solution (0.61 μM) by the **cycHC[8]** up to the 3656 equivalents. Down: plot of the experimental values of absorbance (black crosses) at specific wavelengths and theoretical values obtained from the fitting of association constants (red line). See the values in the main text.

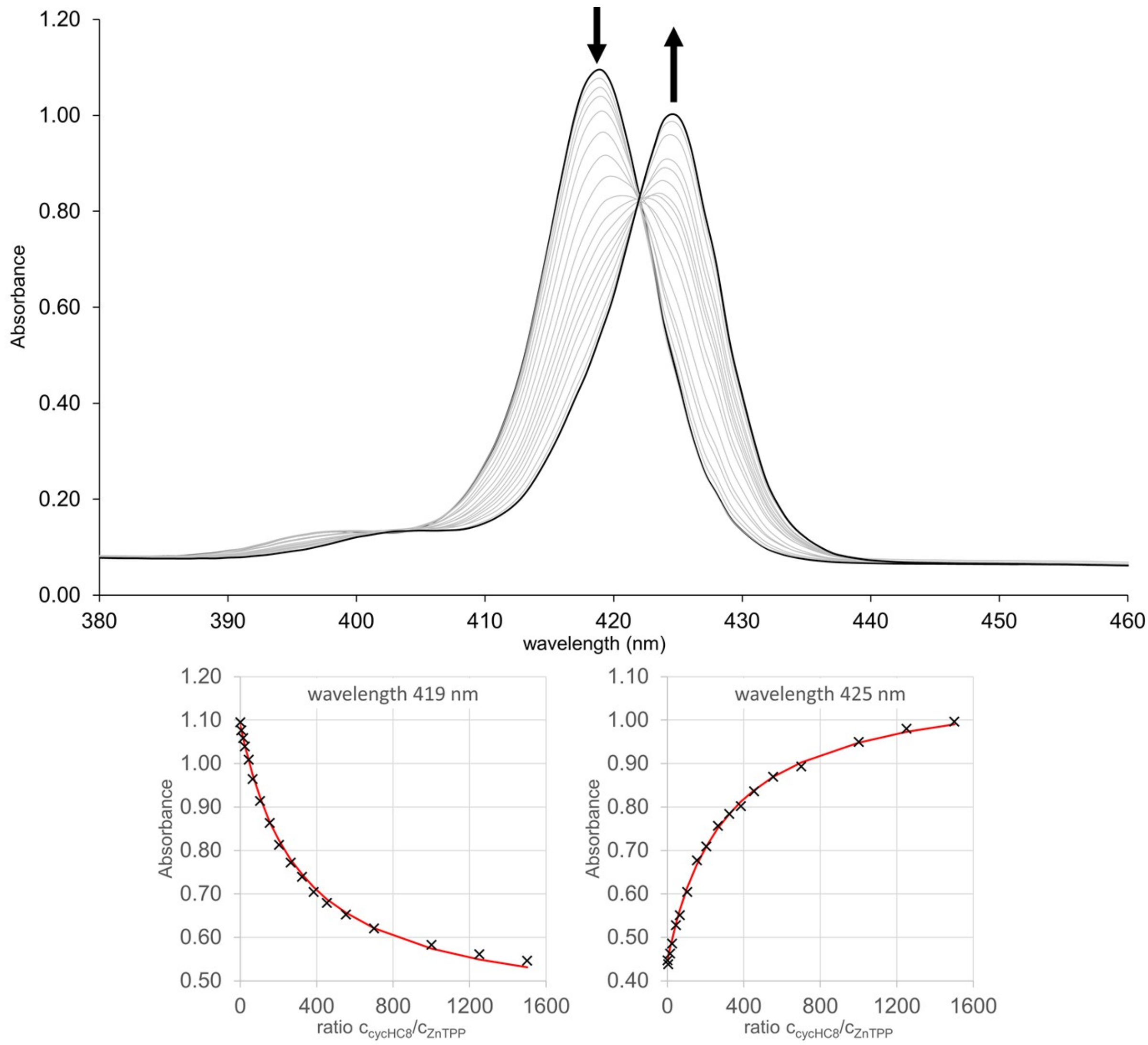

Figure S14. Up: UV-VIS titration of **ZnTPP** solution (1.60 μM) by the **cycHC[8]** up to the 1500 equivalents. Down: plot of the experimental values of absorbance (black crosses) at specific wavelengths and theoretical values obtained from the fitting of association constants (red line). See the values in the main text.

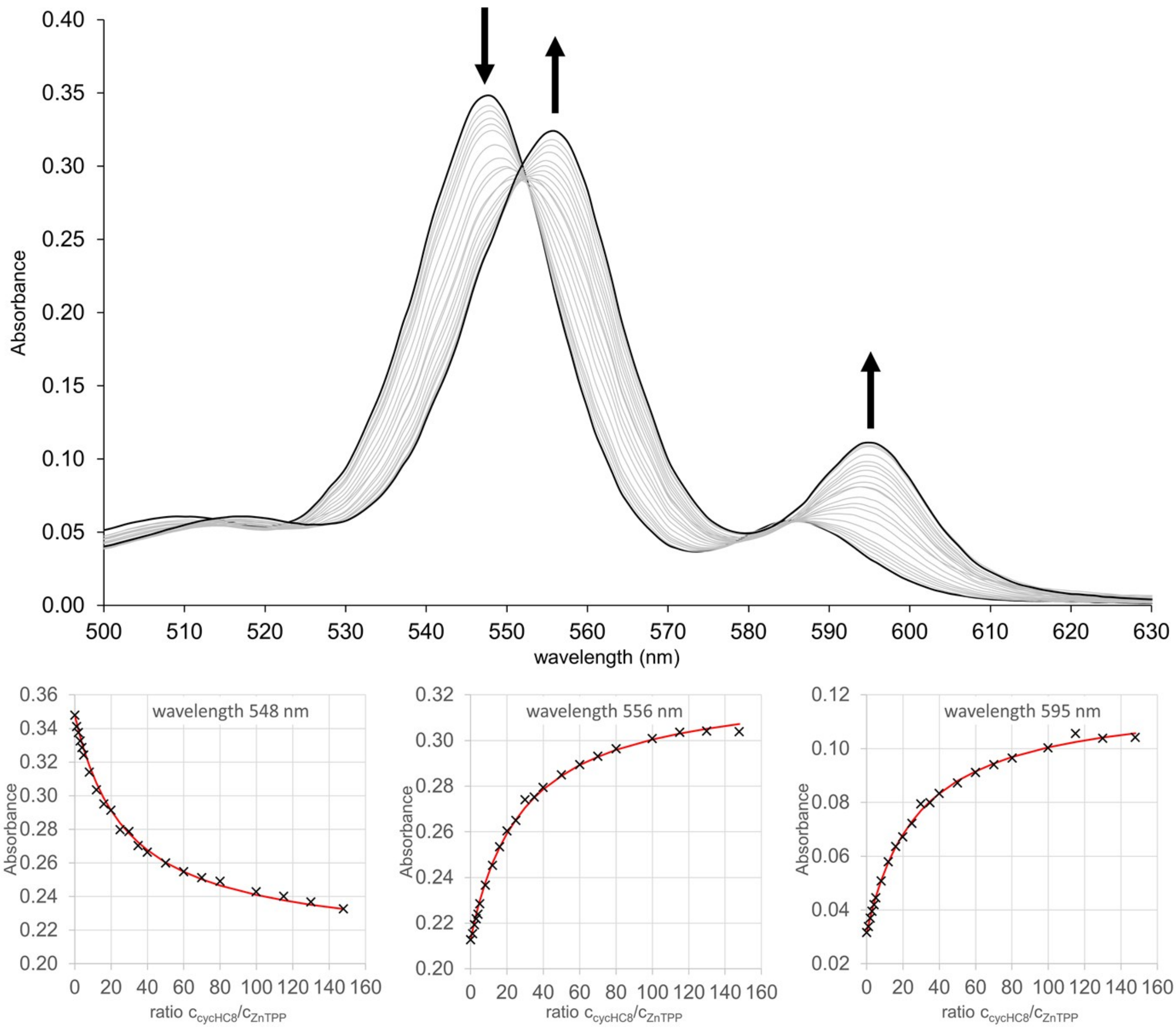

Figure S15. Up: UV-VIS titration of **ZnTPP** solution (17.1 μM) by the **cycHC[8]** up to the 148 equivalents. Down: plot of the experimental values of absorbance (black crosses) at specific wavelengths and theoretical values obtained from the fitting of association constants (red line). See the values in the main text.

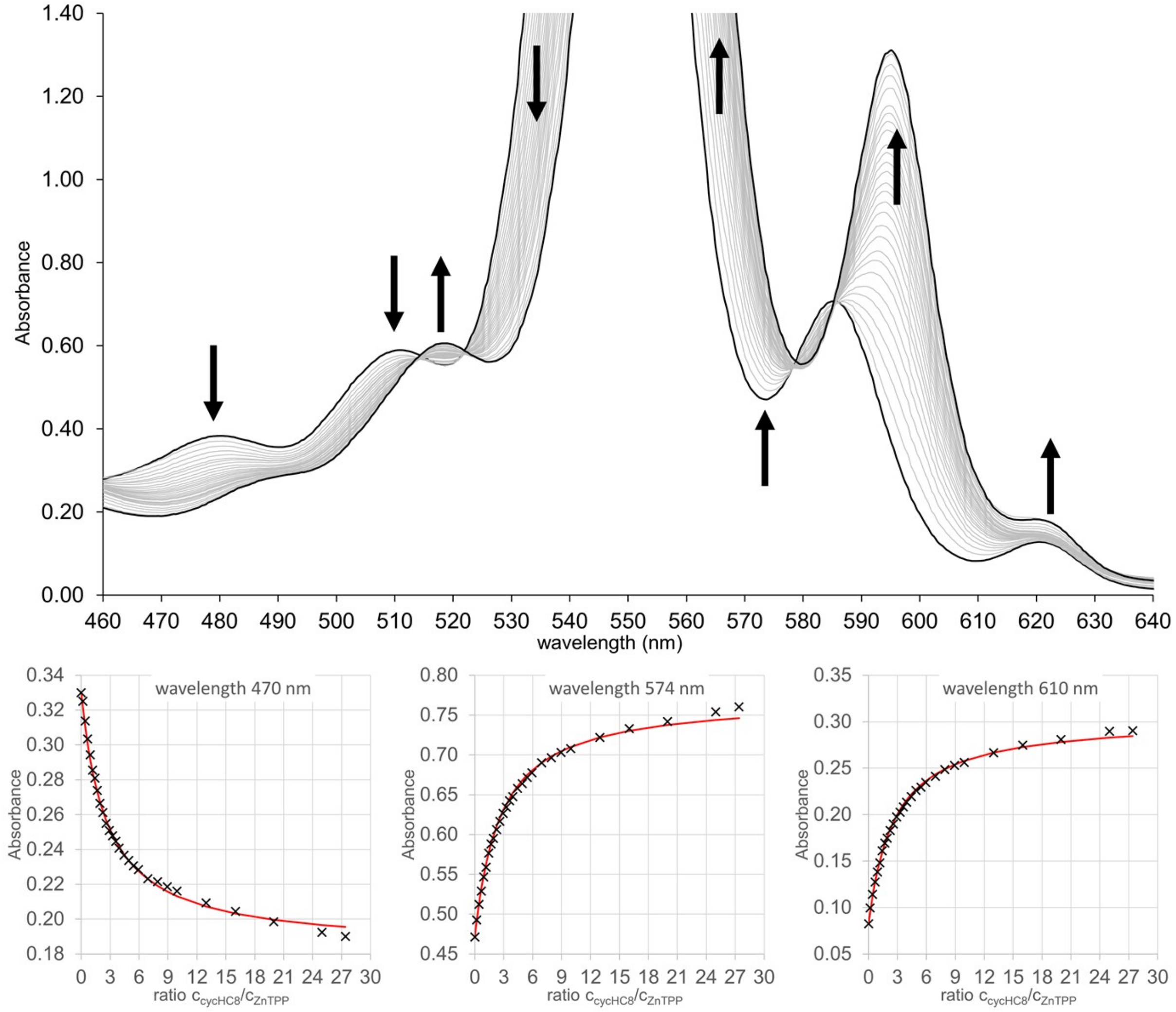

Figure S16. Up: UV-VIS titration of **ZnTPP** solution (190 µM) by the **cycHC[8]** up to the 27.4 equivalents. Down: plot of the experimental values of absorbance (black crosses) at specific wavelengths and theoretical values obtained from the fitting of association constants (red line). See the values in the main text.

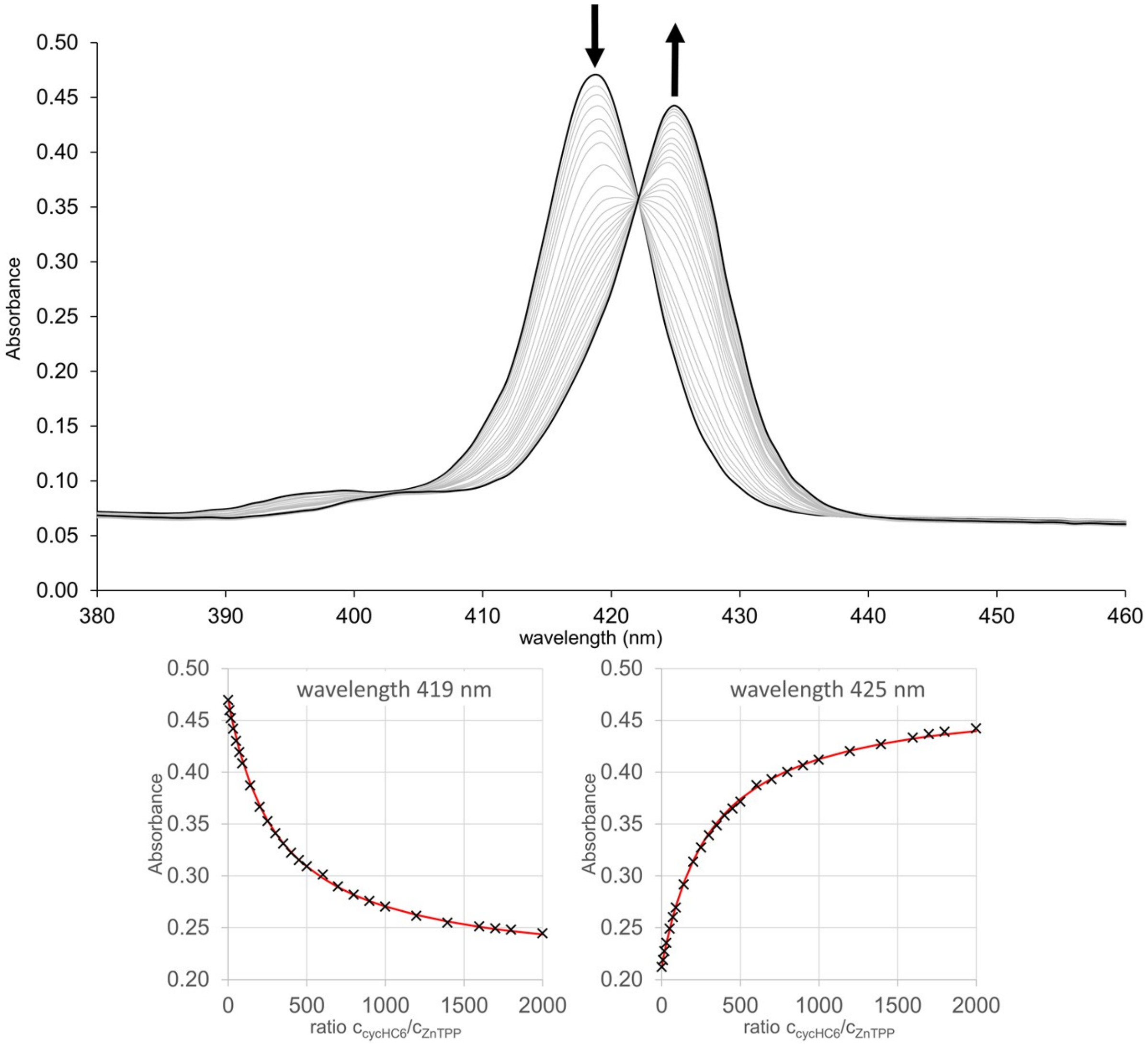

Figure S17. Up: UV-VIS titration of **ZnTPP** solution (0.60 μM) by the **cycHC[6]** up to the 1998 equivalents. Down: plot of the experimental values of absorbance (black crosses) at specific wavelengths and theoretical values obtained from the fitting of association constants (red line). See the values in the main text.

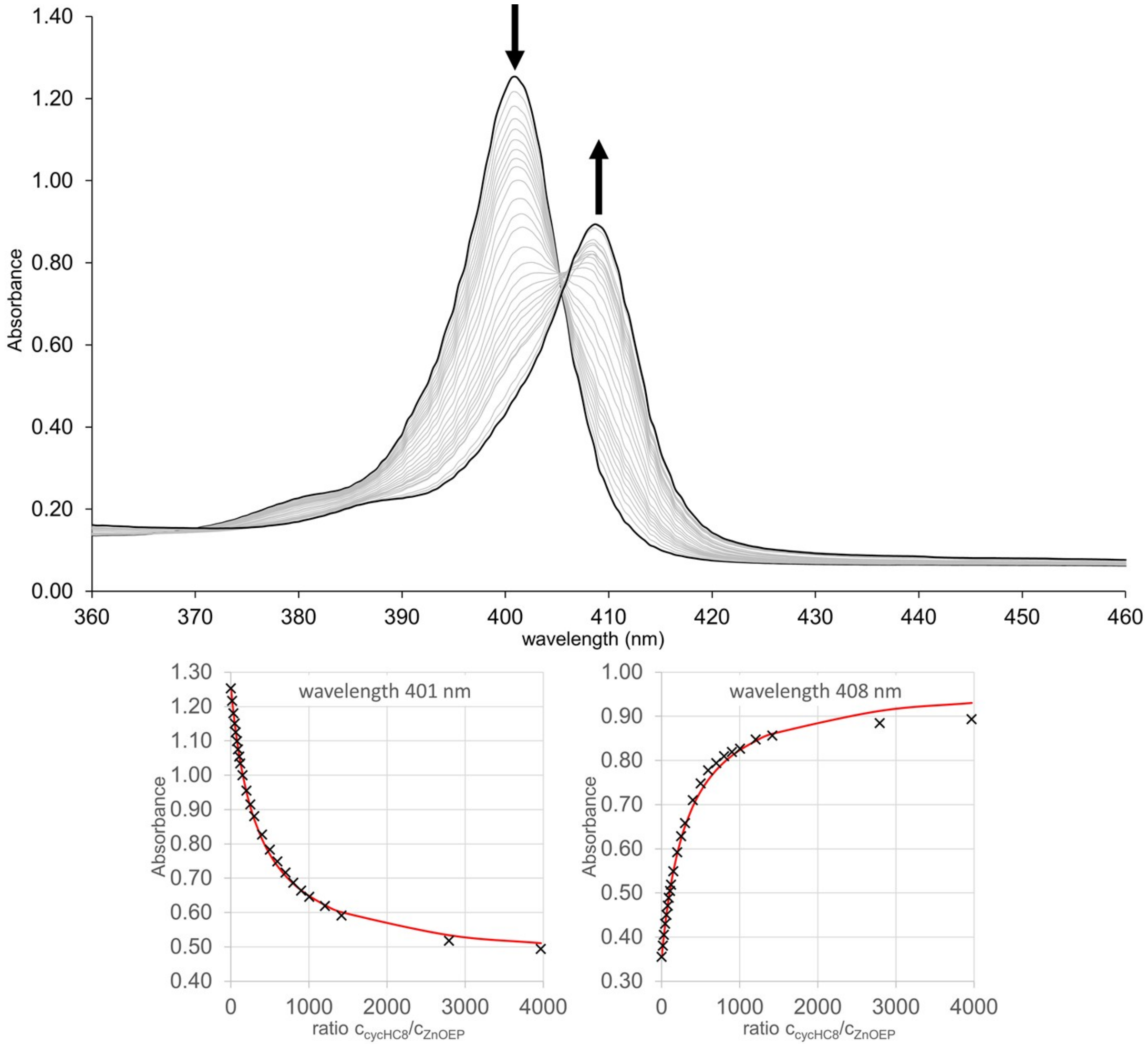

Figure S18. Up: UV-VIS titration of **ZnOEP** solution (3.46 μM) by the **cycHC[8]** up to the 3967 equivalents. Down: plot of the experimental values of absorbance (black crosses) at specific wavelengths and theoretical values obtained from the fitting of association constants (red line). See the values in the main text.

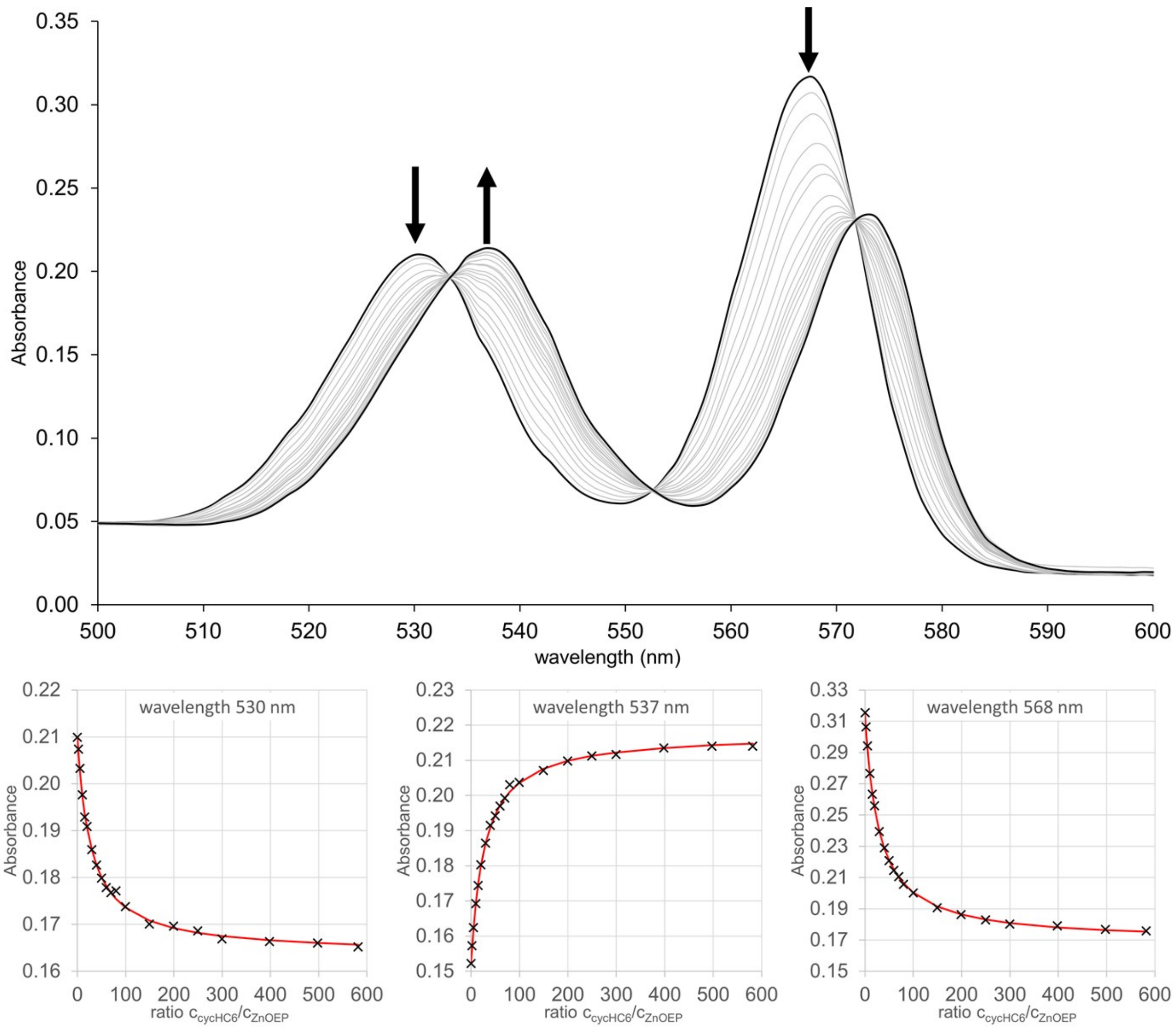

Figure S19. Up: UV-VIS titration of **ZnOEP** solution (12.0 µM) by the **cycHC[6]** up to the 582 equivalents. Down: plot of the experimental values of absorbance (black crosses) at specific wavelengths and theoretical values obtained from the fitting of association constants (red line). See the values in the main text.

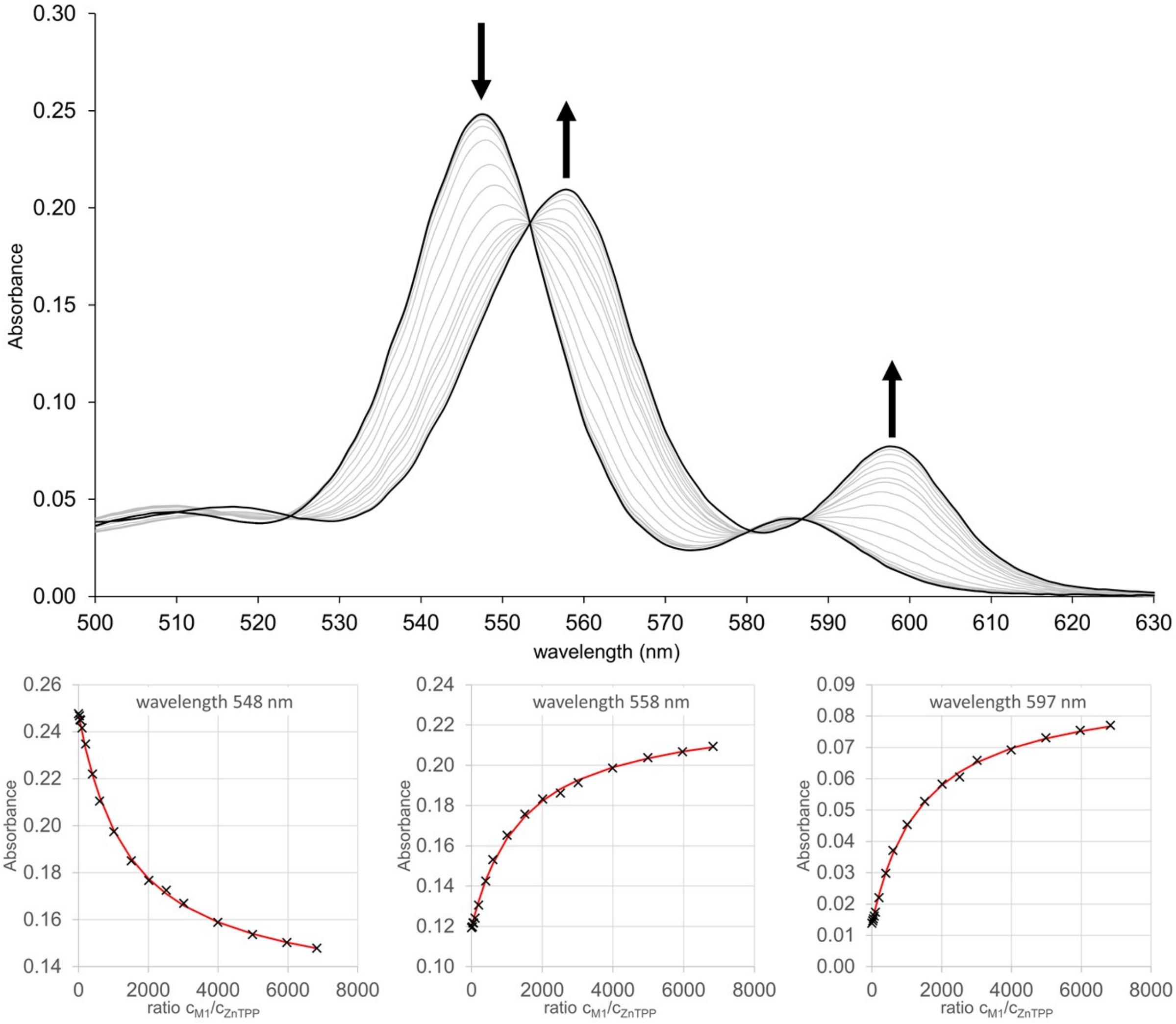

Figure S20. Up: UV-VIS titration of **ZnTPP** solution (12.0 µM) by the **M1** up to the 6830 equivalents. Down: plot of the experimental values of absorbance (black crosses) at specific wavelengths and theoretical values obtained from the fitting of association constants (red line). See the values in the main text.

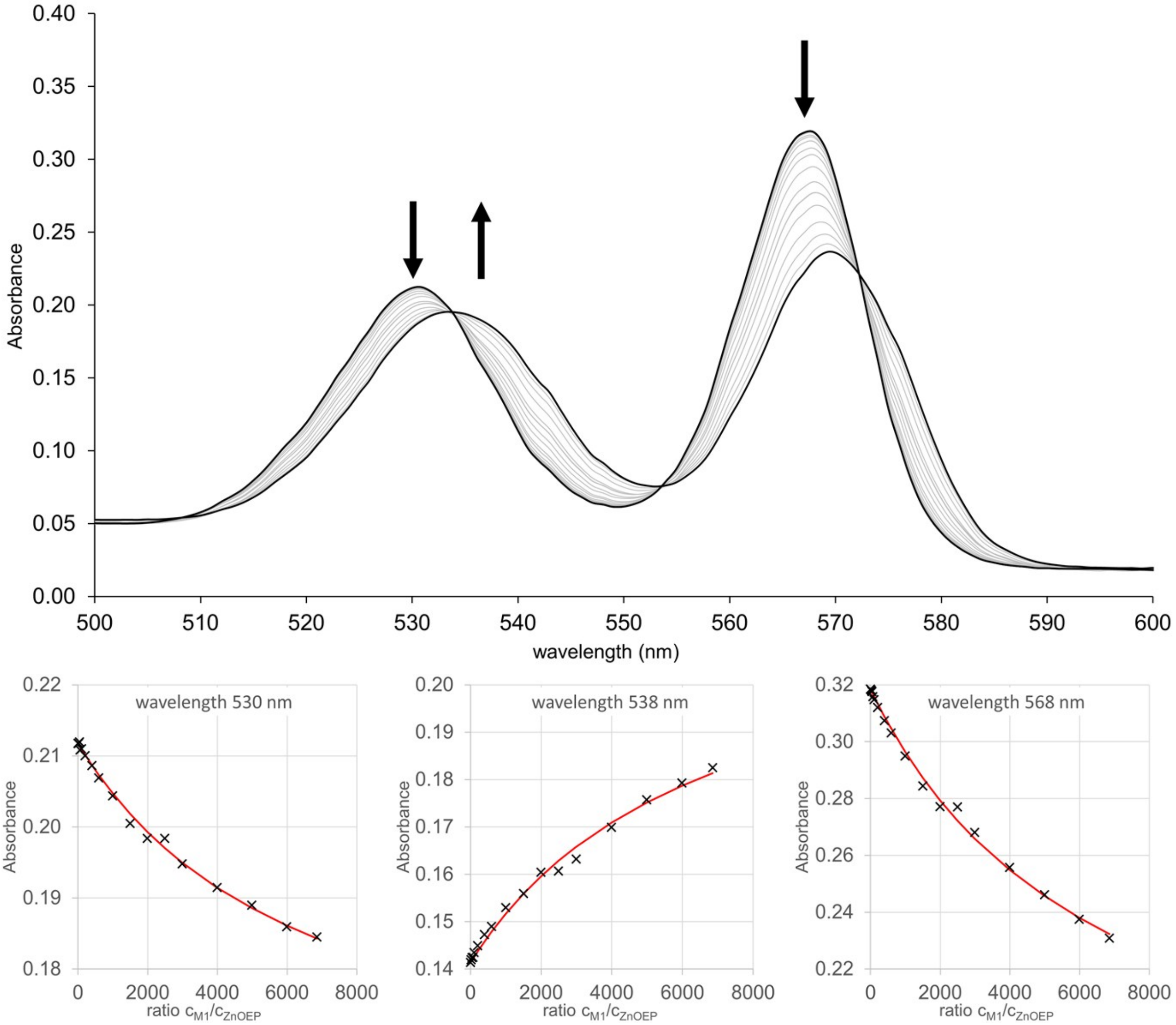

Figure S21. Up: UV-VIS titration of **ZnOEP** solution (12.1 µM) by the **M1** up to the 6853 equivalents. Down: plot of the experimental values of absorbance (black crosses) at specific wavelengths and theoretical values obtained from the fitting of association constants (red line). See the values in the main text.

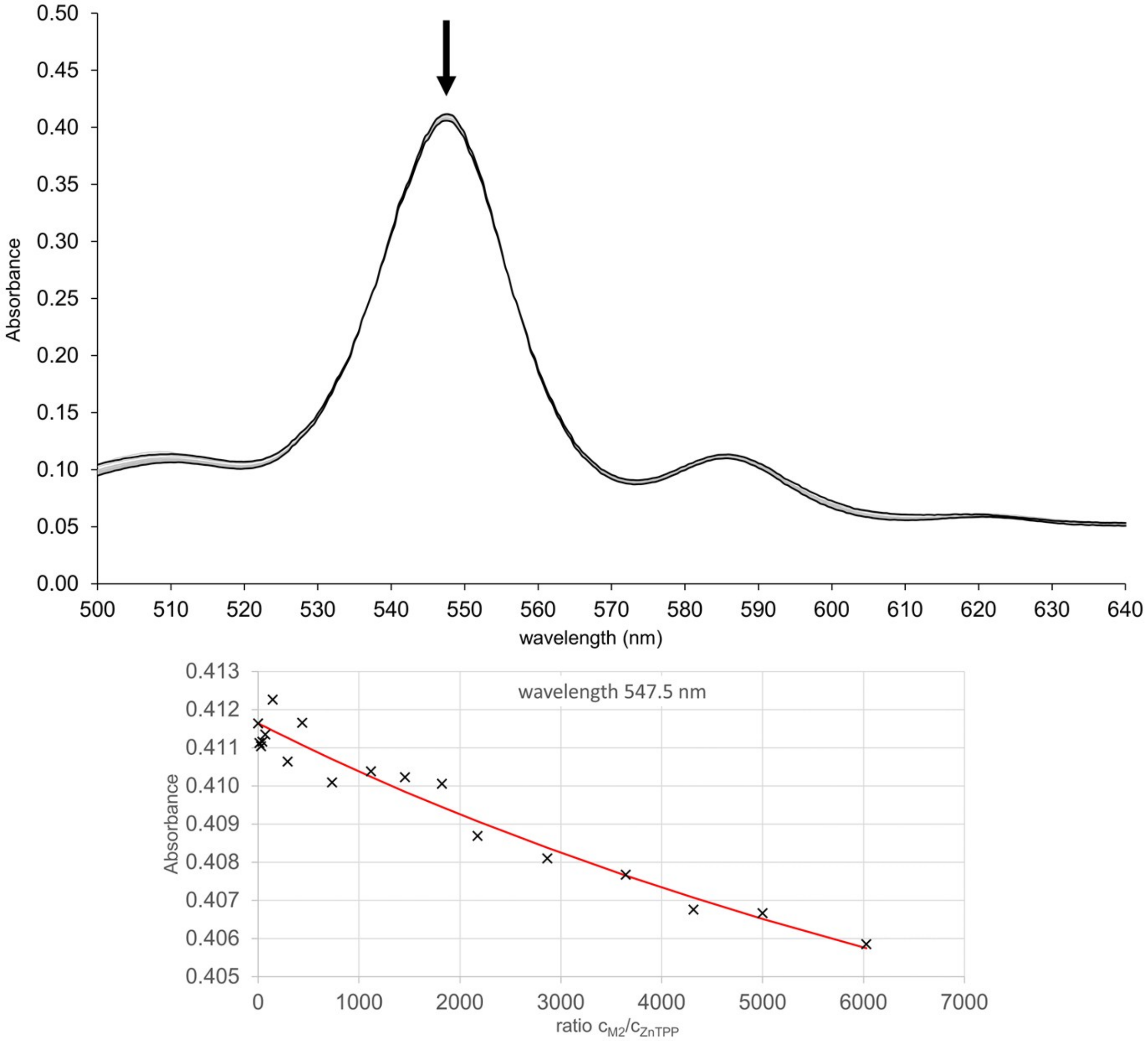

Figure S22. Up: UV-VIS titration of **ZnTPP** solution (16.5 μM) by the **M2** up to the 6028 equivalents. Down: plot of the experimental values of absorbance (black crosses) at specific wavelengths and theoretical values obtained from the fitting of association constants (red line) according to 1:1 binding model from http://supramolecular.org. Very weak association constant $K_1 = 3.7 \pm 0.4$ M^{-1} was obtained.

List of Soret band wavelengths in UV-VIS for used free porphyrins and their complexes with cycHCs in DCM:

λ_{Soret}(**ZnTPP**) = 418.4 nm
λ_{Soret}(**cycHC[6]·ZnTPP**) = 424.7 nm
λ_{Soret}(**cycHC[8]·ZnTPP**) = 424.2 nm
λ_{Soret}(**ZnOEP**) = 400.4 nm
λ_{Soret}(**cycHC[6]·ZnOEP**) = 408.6 nm
λ_{Soret}(**cycHC[8]·ZnOEP**) = 408.2 nm

NMR titrations

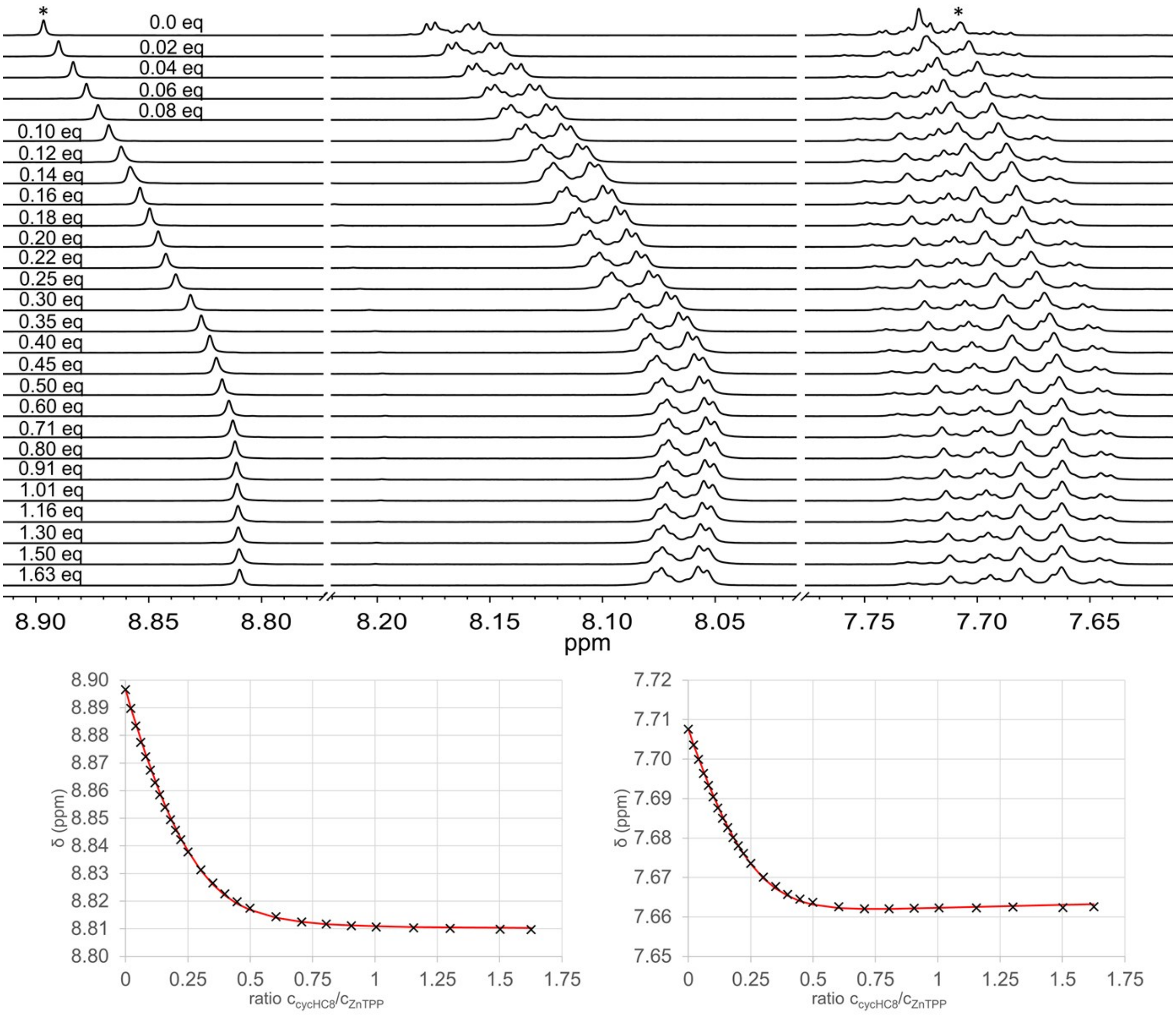

Figure S23. Up: ^{1}H NMR (300 MHz, $CH_2Cl_2/CDCl_3$ - 5%) titration of **ZnTPP** solution (4.96 mM) by the **cycHC[8]** up to the 1.63 equivalents. Followed signals of *β*-H and *m,p*-phenyl H are marked with asterisk (*). Down: plot of the experimental values of chemical shift (black crosses) of **ZnTPP** signals and theoretical values obtained from the fitting of association constants (red line). See the values in the main text.

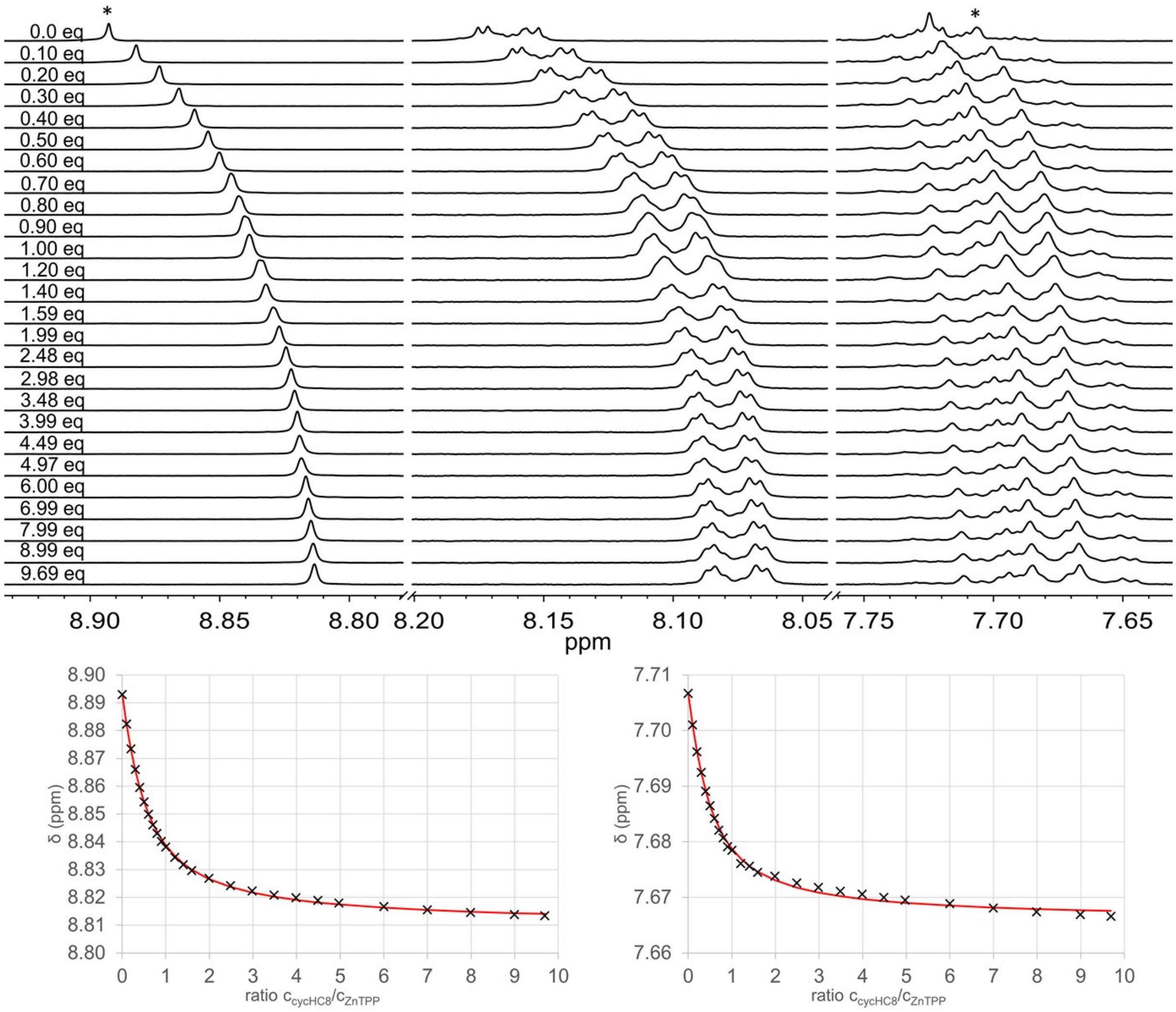

Figure S24. Up: ^{1}H NMR (300 MHz, CH$_2$Cl$_2$/CDCl$_3$ - 5%) titration of **ZnTPP** solution (0.88 mM) by the **cycHC[8]** up to the 9.69 equivalents. Followed signals of *β*-H and *m,p*-phenyl H are marked with asterisk (*). Down: plot of the experimental values of chemical shift (black crosses) of **ZnTPP** signals and theoretical values obtained from the fitting of association constants (red line). See the values in the main text.

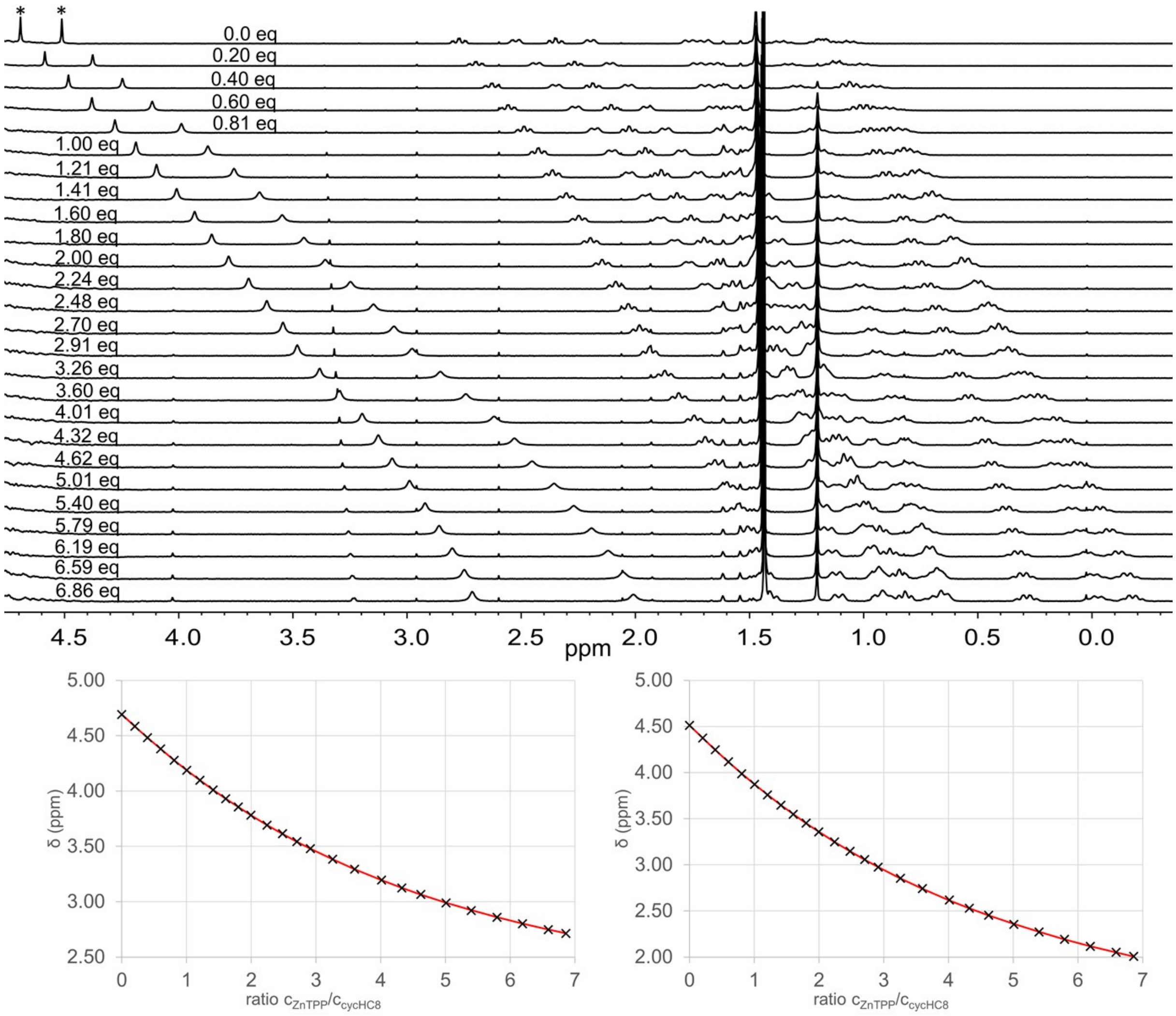

Figure S25. Up: ^{1}H NMR (300 MHz, $CH_2Cl_2/CDCl_3$ - 5%) titration of **cycHC[8]** solution (0.61 mM) by the **ZnTPP** up to the 6.86 equivalents. Followed signals of methylene bridges are marked with asterisk (*). Down: plot of the experimental values of chemical shift (black crosses) of **cycHC[8]** signals and theoretical values obtained from the fitting of association constants (red line). See the values in the main text.

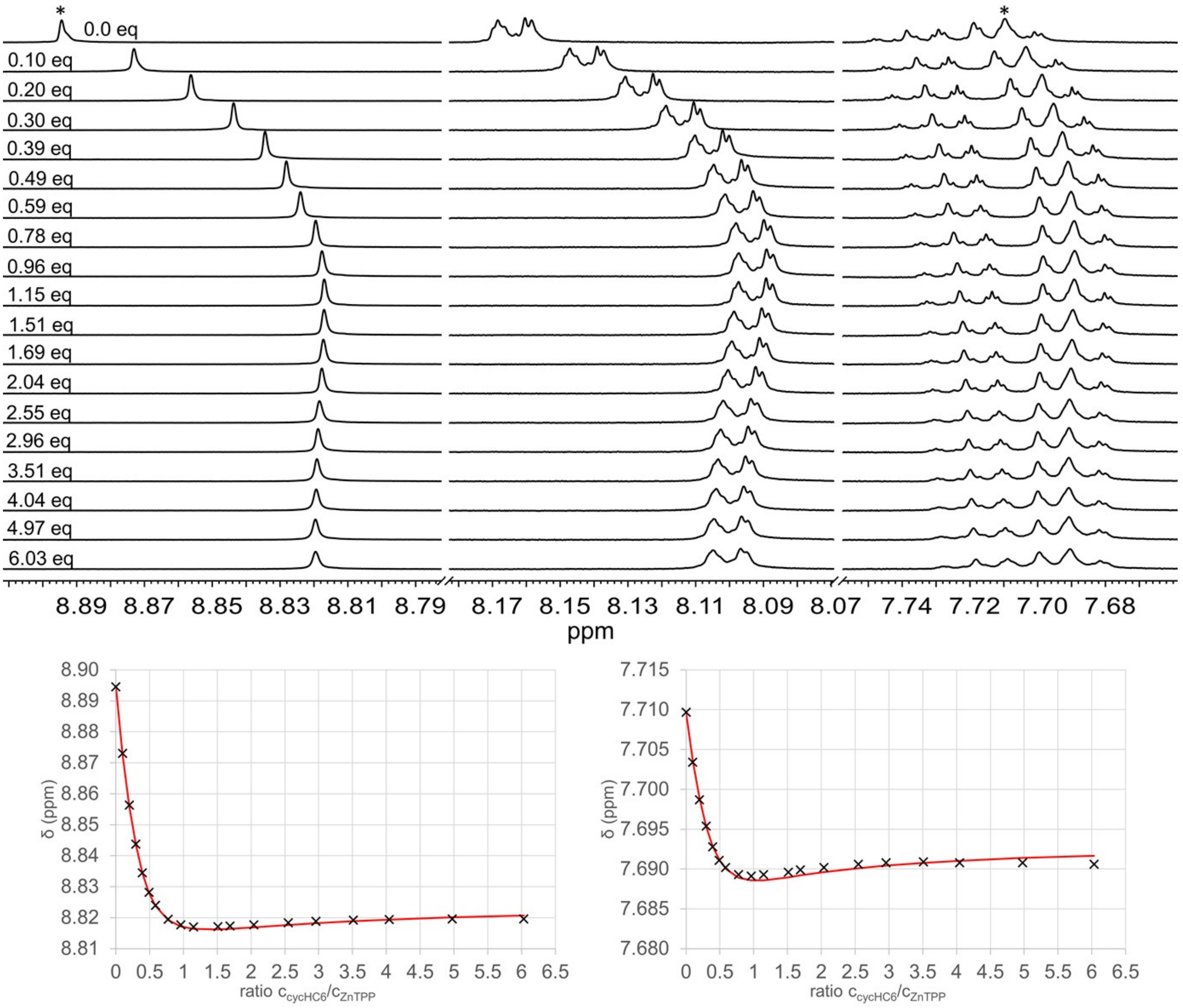

Figure S26. Up: ^{1}H NMR (800 MHz, $CH_2Cl_2/CDCl_3$ - 5%) titration of **ZnTPP** solution (1.01 mM) by the **cycHC[6]** up to the 6.03 equivalents. Followed signals of *β*-H and *m,p*-phenyl H are marked with asterisk (*). Down: plot of the experimental values of chemical shift (black crosses) of **ZnTPP** signals and theoretical values obtained from the fitting of association constants (red line). See the values in the main text.

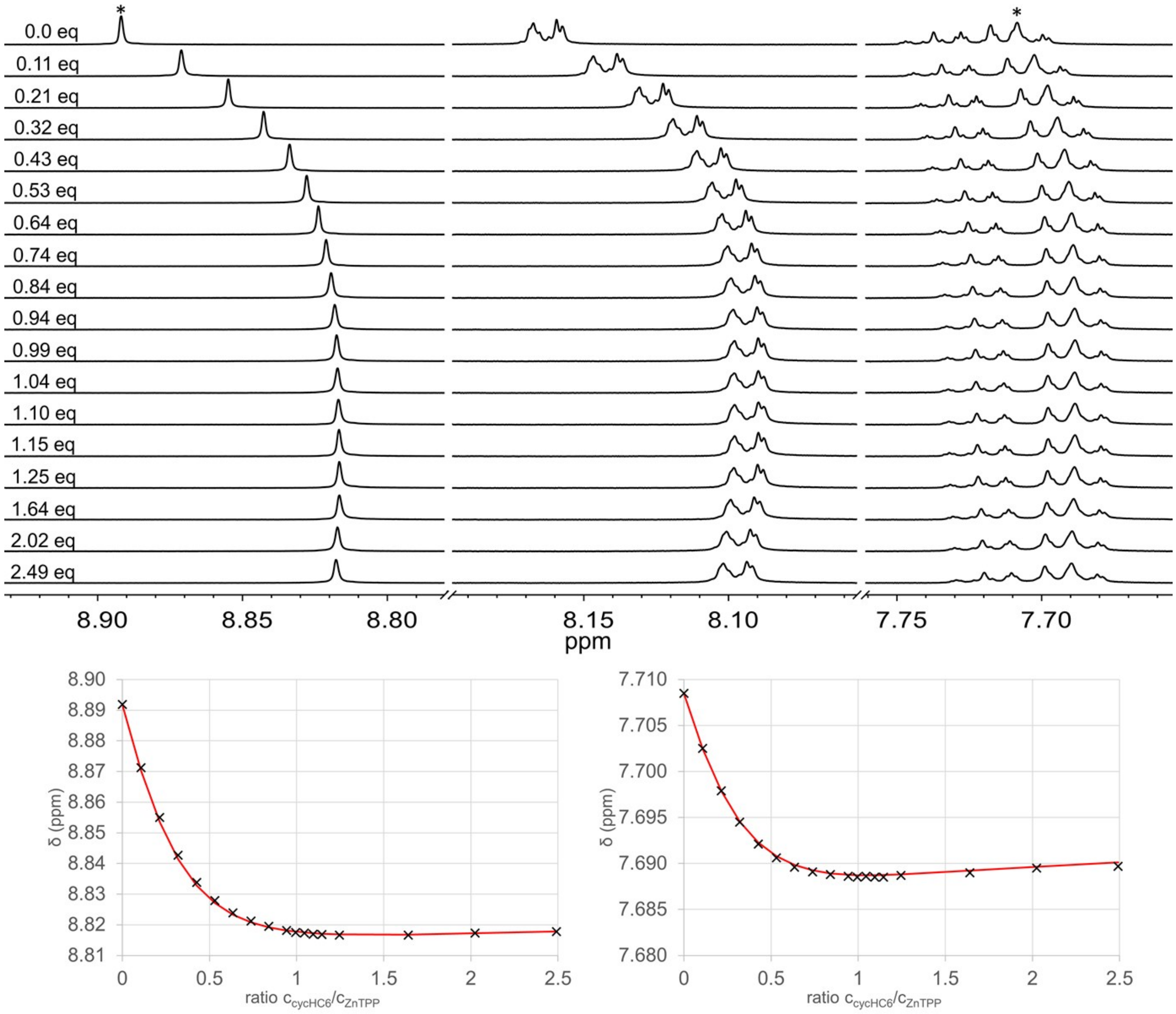

Figure S27. Up: ^{1}H NMR (800 MHz, $CH_2Cl_2/CDCl_3$ - 5%) titration of **ZnTPP** solution (0.94 mM) by the **cycHC[6]** up to the 2.49 equivalents. Followed signals of *β*-H and *m,p*-phenyl H are marked with asterisk (*). Down: plot of the experimental values of chemical shift (black crosses) of **ZnTPP** signals and theoretical values obtained from the fitting of association constants (red line). See the values in the main text.

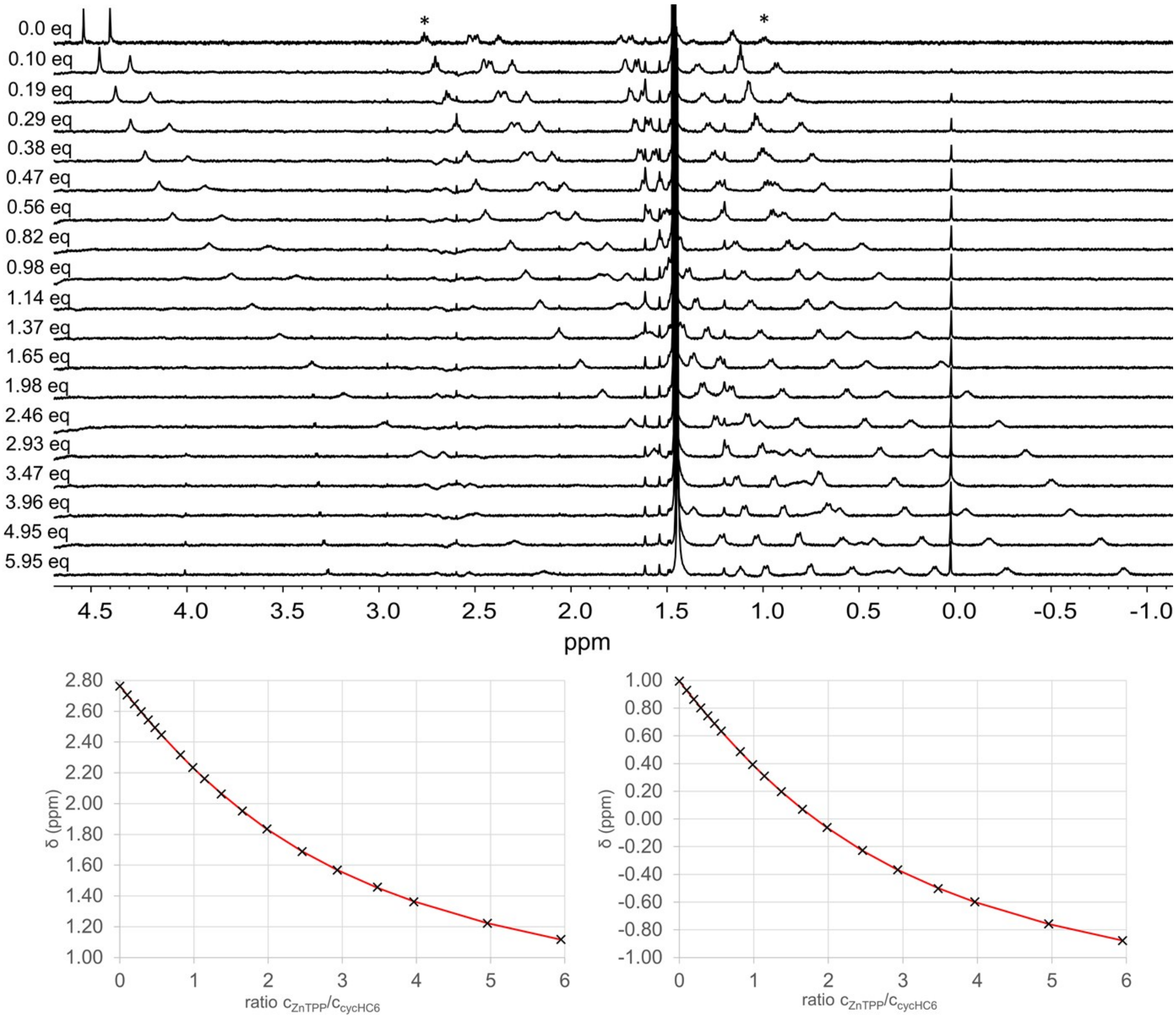

Figure S28. Up: ^{1}H NMR (800 MHz, $CH_2Cl_2/CDCl_3$ - 5%) titration of **cycHC[6]** solution (0.56 mM) by the **ZnTPP** up to the 5.93 equivalents. Followed signals of C-H(out) and one of *axial* H of cyclohexano ring are marked with asterisk (*). Down: plot of the experimental values of chemical shift (black crosses) of **cycHC[6]** signals and theoretical values obtained from the fitting of association constants (red line). See the values in the main text.

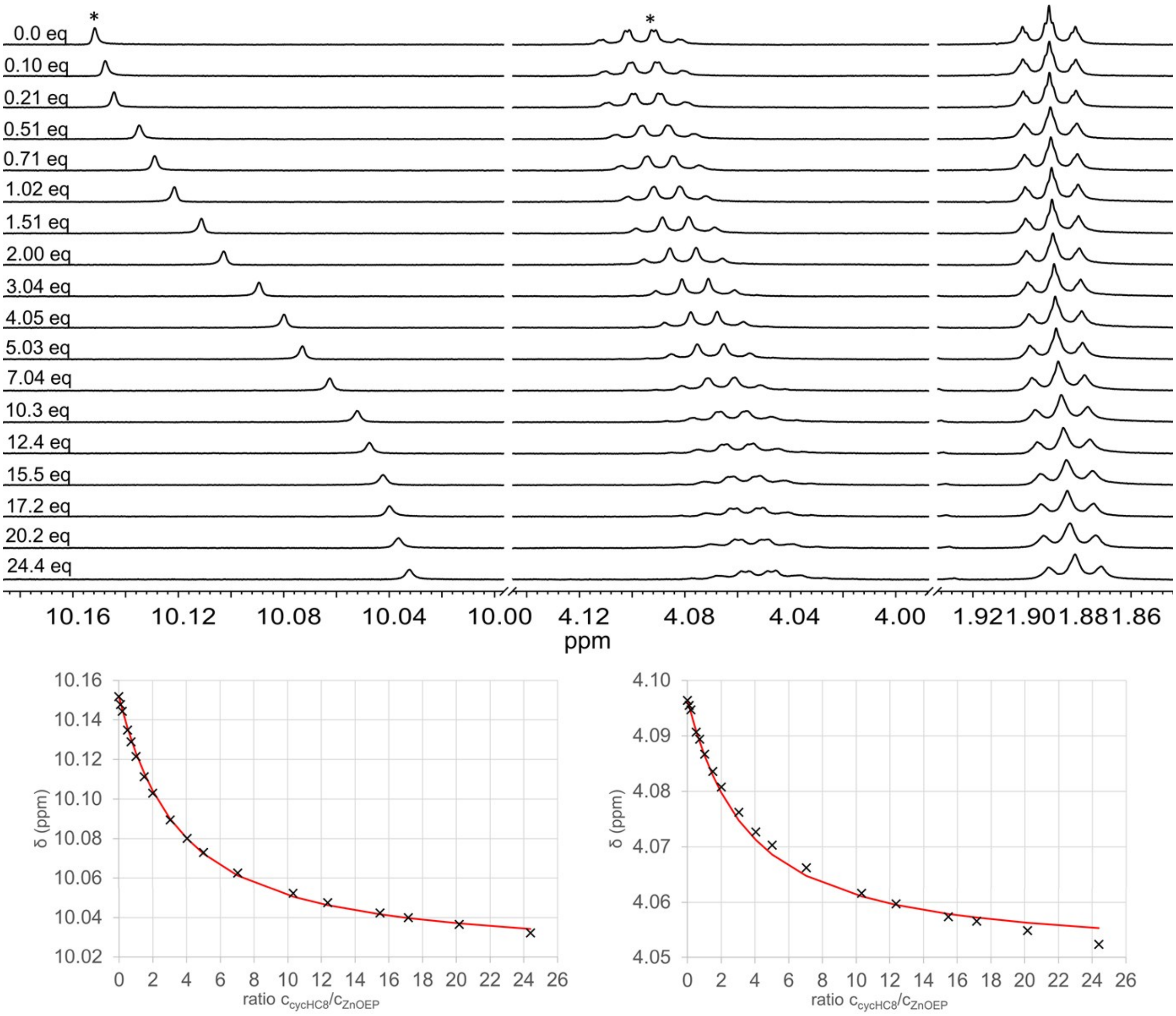

Figure S29. Up: ^{1}H NMR (800 MHz, $CH_2Cl_2/CDCl_3$ - 5%) titration of **ZnOEP** solution (0.49 mM) by the **cycHC[8]** up to the 24.4 equivalents. Followed signals of *meso*-H and CH_2 are marked with asterisk (*). Down: plot of the experimental values of chemical shift (black crosses) of **ZnOEP** signals and theoretical values obtained from the fitting of association constants (red line). See the values in the main text.

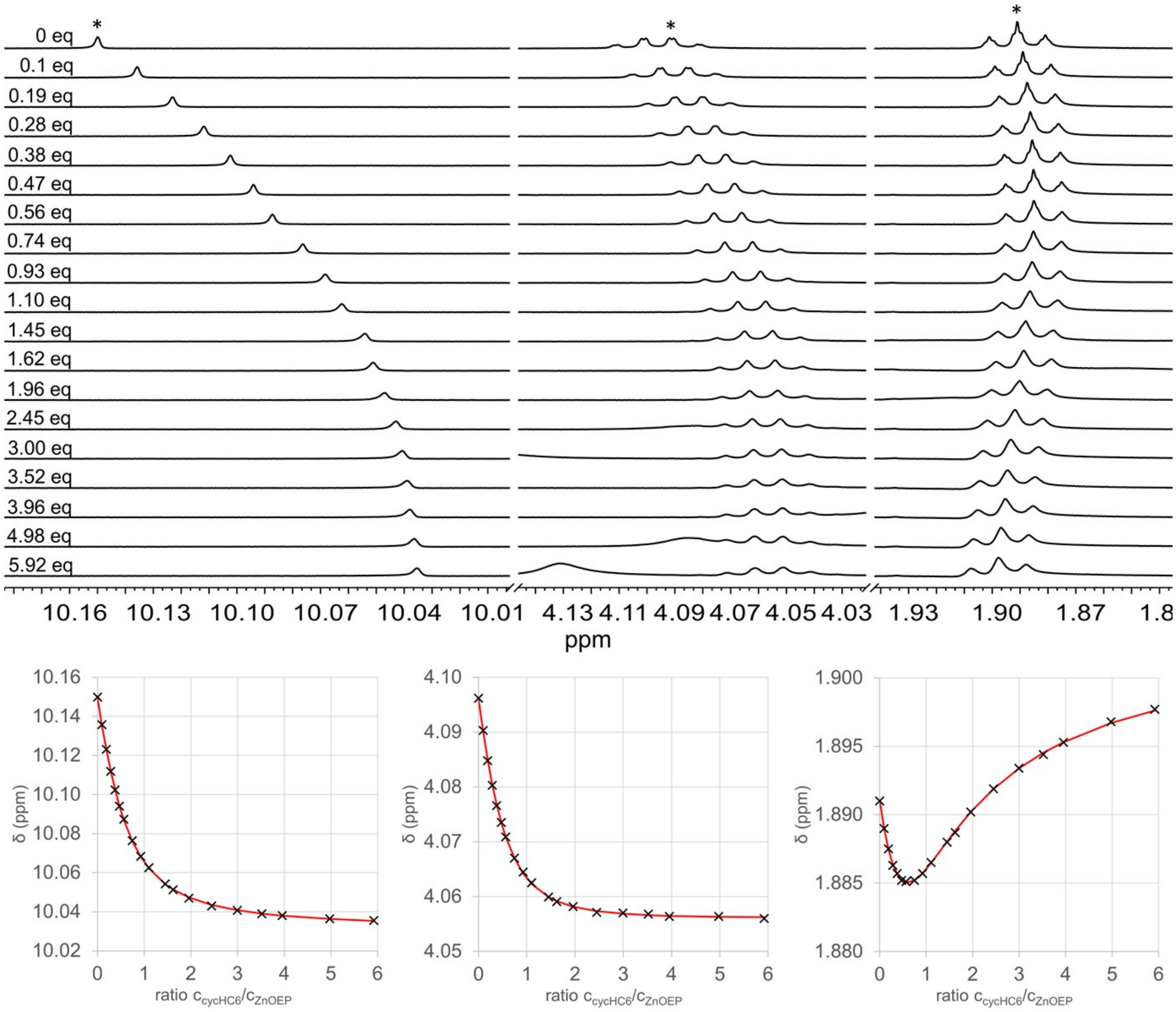

Figure S30. Up: ^{1}H NMR (800 MHz, $CH_2Cl_2/CDCl_3$ - 5%) titration of **ZnOEP** solution (0.52 mM) by the **cycHC[6]** up to the 5.92 equivalents. Followed signals of **ZnOEP** (*meso*-H, CH_2, CH_3) are marked with asterisk (*). Down: plot of the experimental values of chemical shift (black crosses) of **ZnOEP** signals and theoretical values obtained from the fitting of association constants (red line). See the values in the main text.

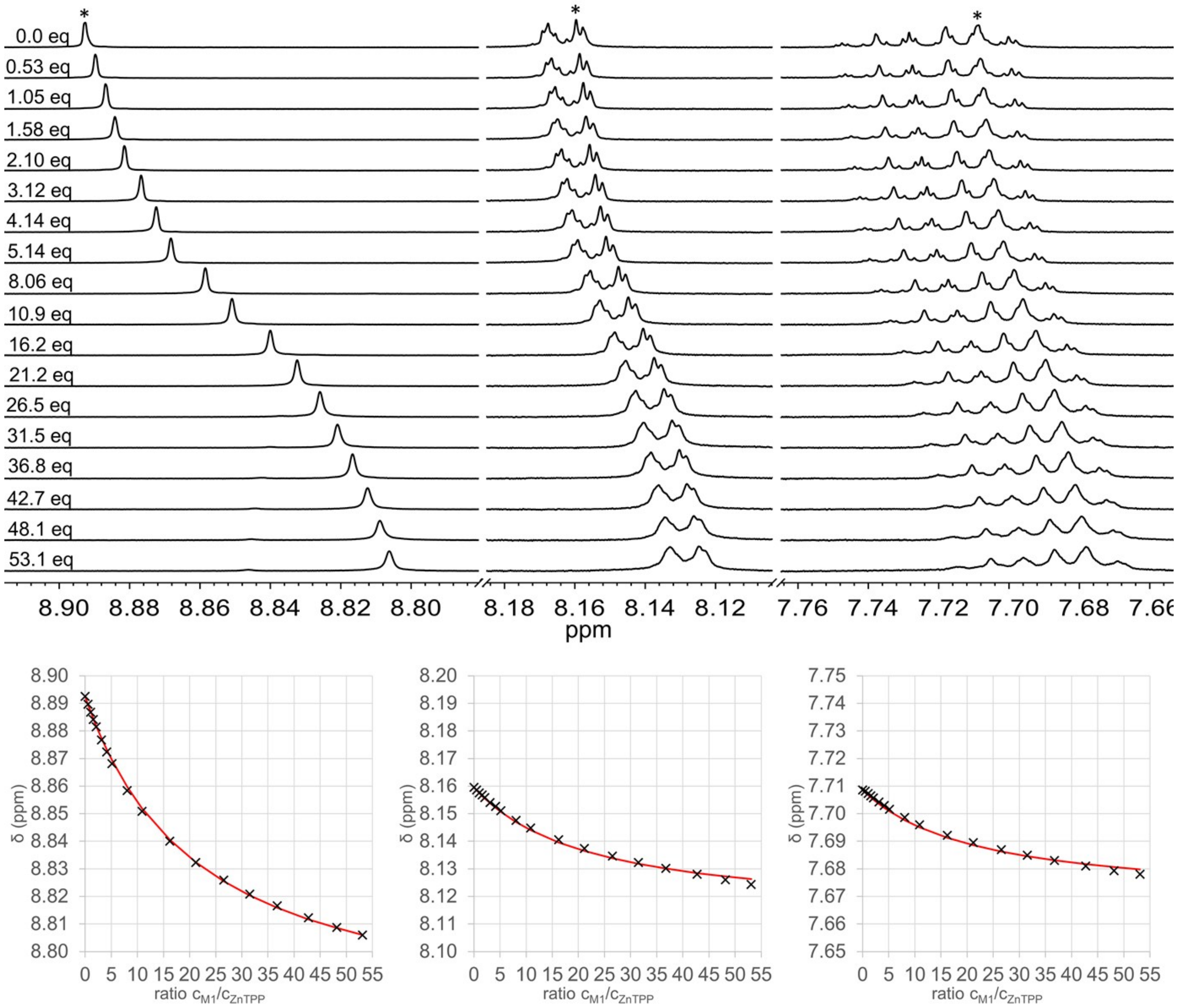

Figure S31. Up: ^{1}H NMR (800 MHz, $CH_2Cl_2/CDCl_3$ - 5%) titration of **ZnTPP** solution (0.94 mM) by the **M1** up to the 53.1 equivalents. Followed signals of **ZnTPP** (*β*-H, *o*-phenyl H, *m,p*-phenyl H) are marked with asterisk (*). Down: plot of the experimental values of chemical shift (black crosses) of **ZnTPP** signals and theoretical values obtained from the fitting of association constants (red line). See the values in the main text.

ITC measurements

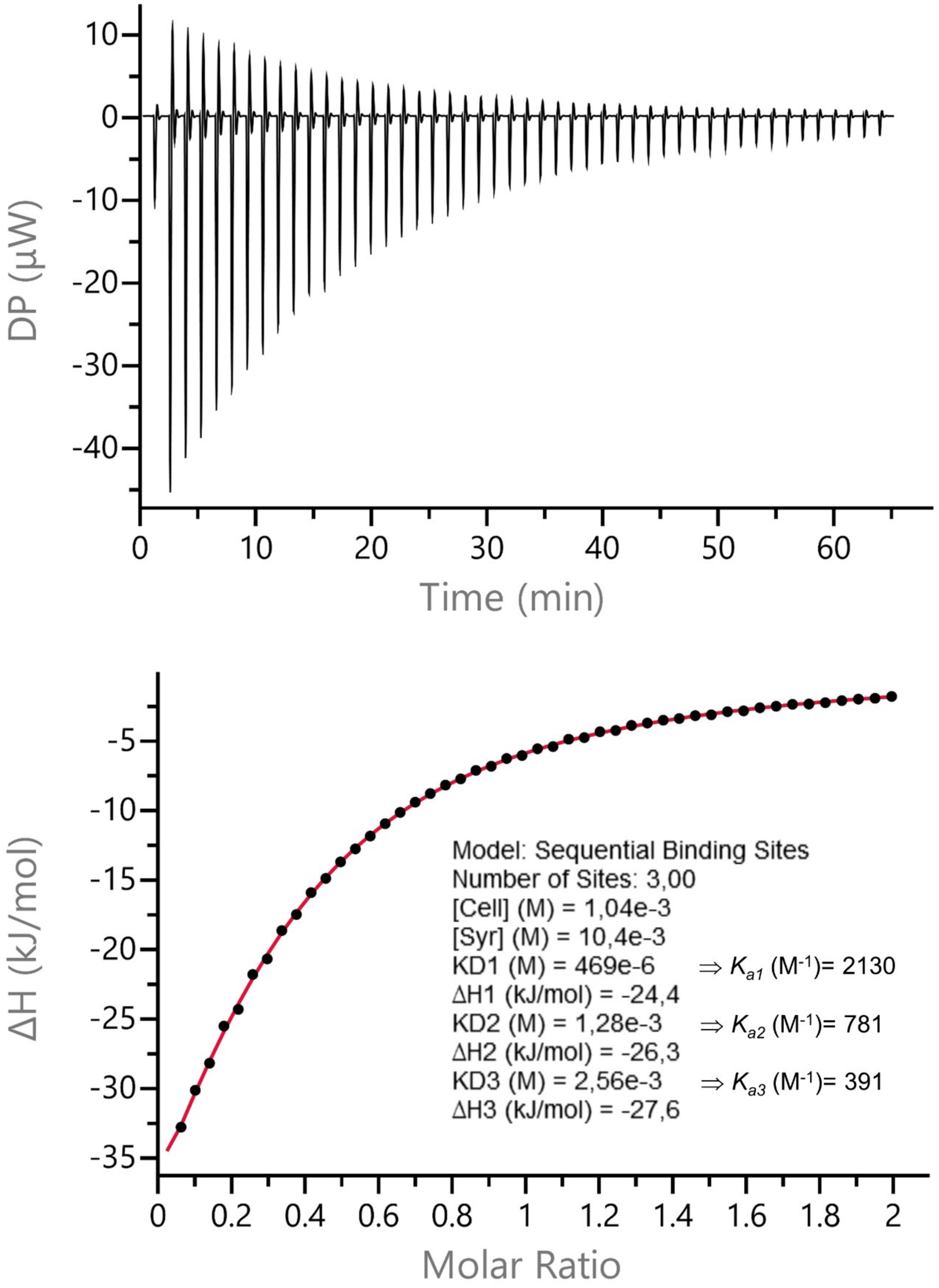

Figure S32. Top: ITC data obtained from the sequential injections of 0.8 μL of **cycHC[8]** solution (10.4 mM) to **ZnTPP** (1.04 mM). Bottom: plot of the total heat released as a function of total ligand concentration for the titration shown in the upper panel. The red solid line represent least-square fit of the data.

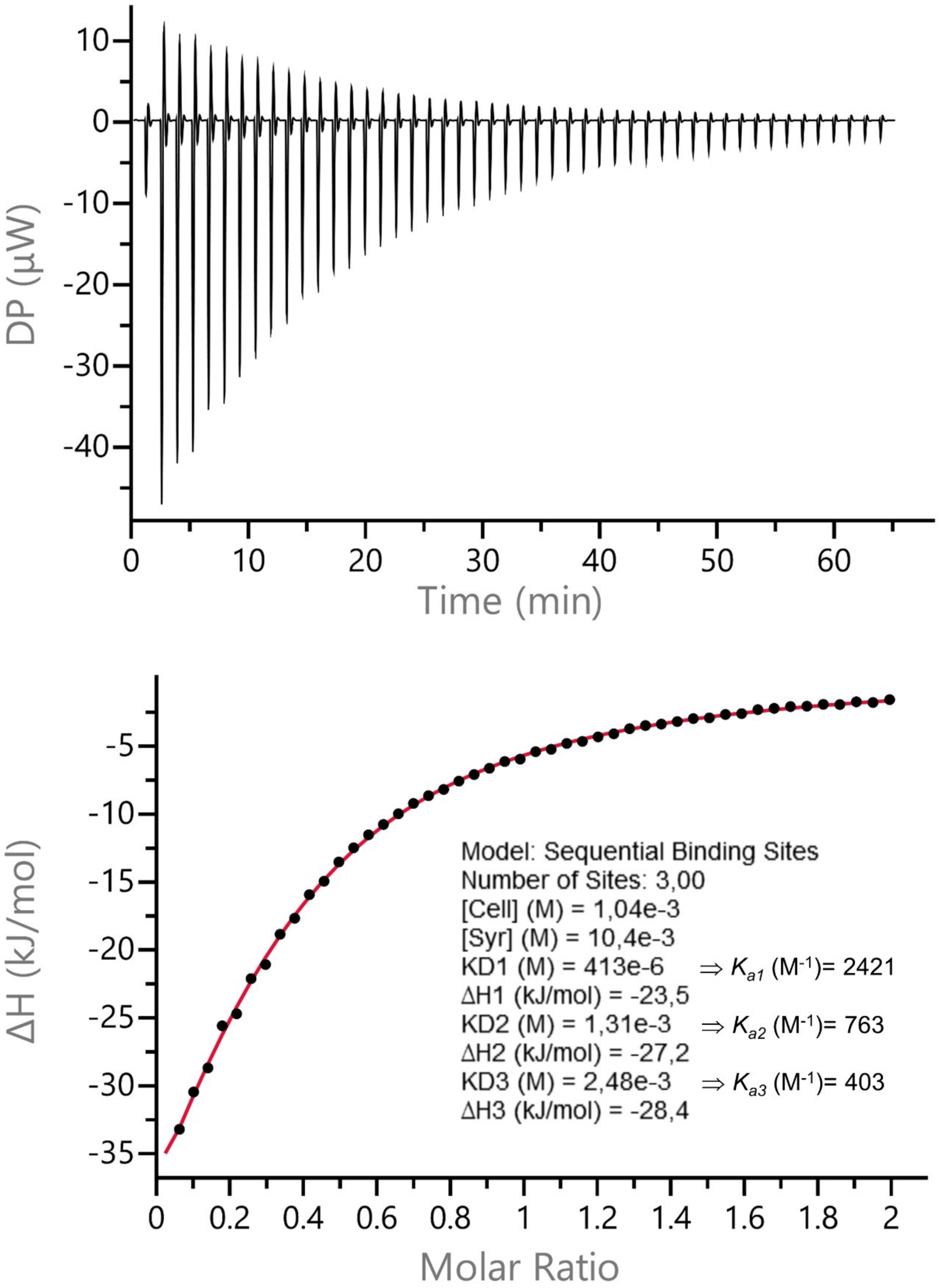

Model: Sequential Binding Sites
Number of Sites: 3,00
[Cell] (M) = 1,04e-3
[Syr] (M) = 10,4e-3
KD1 (M) = 413e-6 ⇒ K_{a1} (M^{-1})= 2421
ΔH1 (kJ/mol) = -23,5
KD2 (M) = 1,31e-3 ⇒ K_{a2} (M^{-1})= 763
ΔH2 (kJ/mol) = -27,2
KD3 (M) = 2,48e-3 ⇒ K_{a3} (M^{-1})= 403
ΔH3 (kJ/mol) = -28,4

Figure S33. Top: ITC data obtained from the sequential injections of 0.8 μL of **cycHC[8]** solution (10.4 mM) to **ZnTPP** (1.04 mM). Bottom: plot of the total heat released as a function of total ligand concentration for the titration shown in the upper panel. The red solid line represent least-square fit of the data.

Job plot experiment

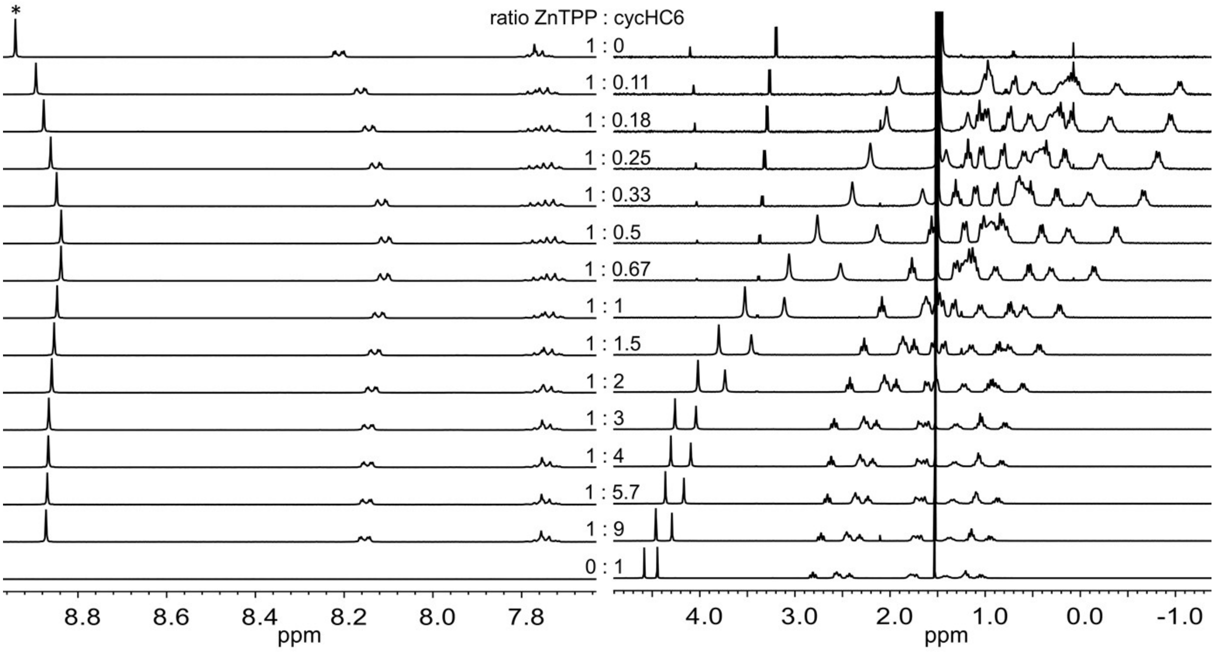

Figure S34. ^{1}H NMR spectra (300 MHz, CD_2Cl_2) of Job's plot experiment for the system containing **ZnTPP** and **cycHC[6]**, overall concentration of components is 4.7 mM in all samples. Followed signal of **ZnTPP** β-H is marked with asterisk (*).

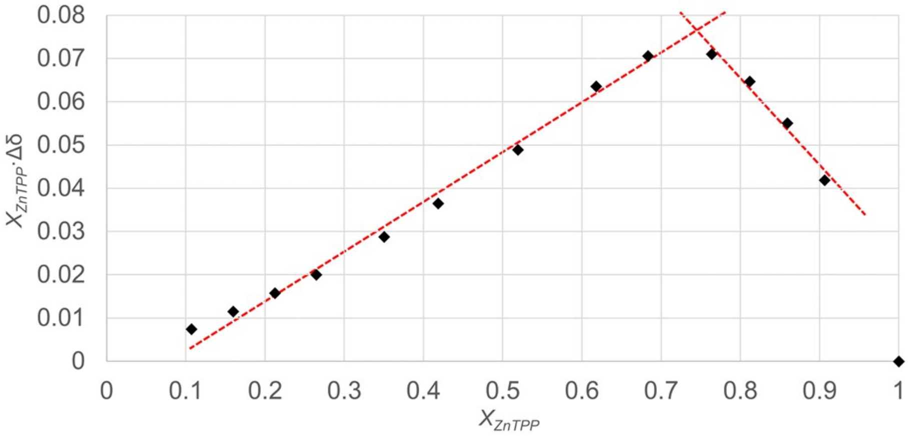

Figure S35. Result of the Job's plot experiment for the system containing **ZnTPP** and **cycHC[6]**, overall concentration of components is 4.7 mM in all samples. The maxima of obtained curve is at 0.75 mole fraction of **ZnTPP** which supports 3:1 (**ZnTPP**: **cycHC[6]**) model of binding.

Variable temperature NMR

Variable temperature ^{1}H NMR spectra were recorded on a 800.13 MHz spectrometer, using evaporated liquid nitrogen for cooling to achieve the desired temperatures, for a 1:2 mixture of **cycHC[6]** and **ZnTPP** (1.1 mM) and similarly **cycHC[8]** and **ZnTPP** (1.9 mM) to see whether it would be possible to lower the temperature to attain below coalescence spectra. Cooling to 230 K demonstrates that for both samples the **cycHC** signals have started to broaden, indicating slowing down of exchange between the interacting molecules. The data show that 230 K is still above the coalescence temperature for both samples with more pronounced signal broadening for **cycHC[6]** as opposed to **cycHC[8]**.

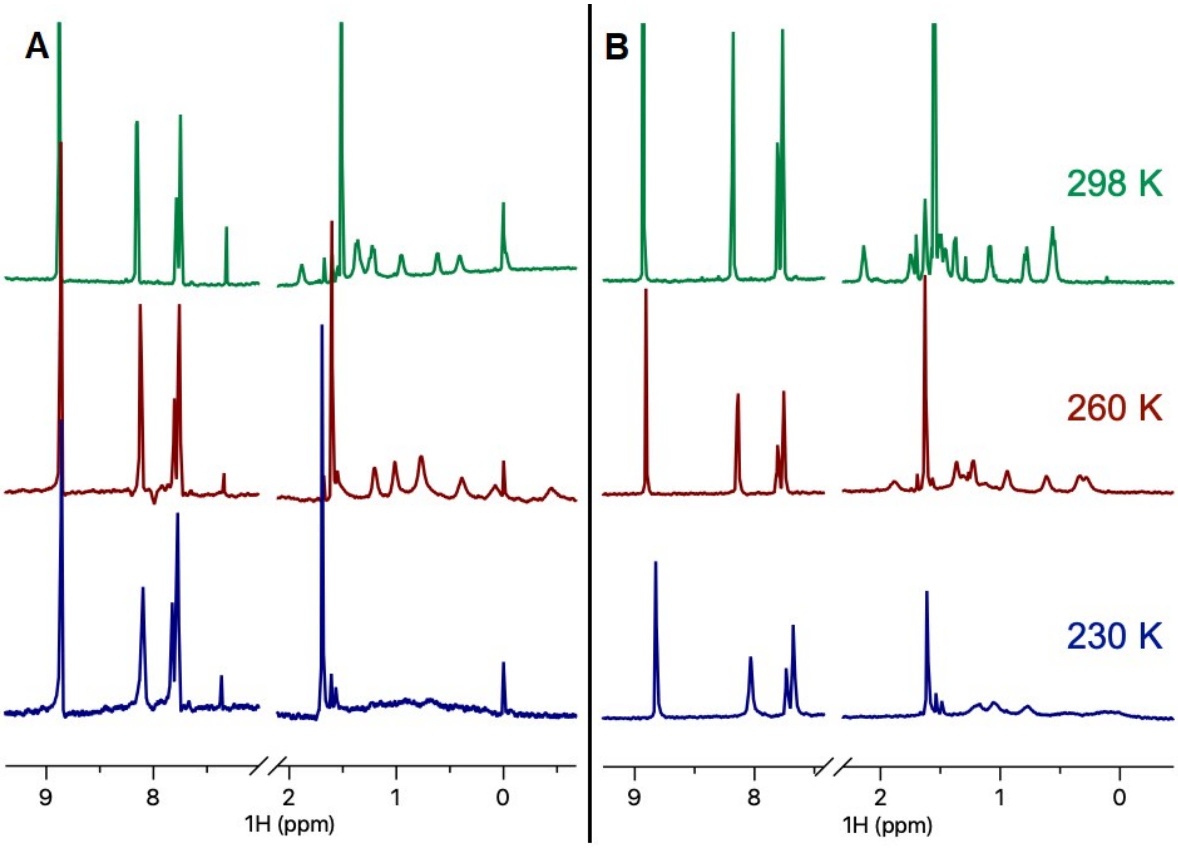

Figure S36. Variable temperature ^{1}H NMR (800 MHz, $CH_2Cl_2/CDCl_3$ - 5%) spectra for **cycHC[6]** and **ZnTPP** (A) and **cycHC[8]** and **ZnTPP** (B) demonstrating exchange above coalescence at all temperatures.

6. Single Crystal X-ray diffraction analysis

General

Single crystal X-ray diffraction data was collected at 123 K on Rigaku Compact HomeLab diffractometer, equipped with a Saturn 944 HG CCD detector and Oxford Cryostream cooling system using monochromatic Cu-*Kα* radiation (1.54178 Å) from a MicroMax$^{\text{TM}}$-003 sealed tube microfocus X-ray source. The strategy of data collections was calculated and implemented through the program package *HKL-3000*.[14] Data was collected using ω-scans. CrysAlisPro [15] was used for data reduction and empirical absorption correction using spherical harmonics implemented in *SCALE3 ABSPACK* scaling algorithm.[16] The structures were solved using *SHELXT* [17] and refined by full-matrix least-squares method against F^2 with *SHELXL-2016* [18] through *OLEX2* program package.[19] All non-hydrogen atoms were refined with anisotropic atomic displacement parameters. Hydrogen atoms attached to carbon atoms were treated as riding atoms, using isotropic displacement parameters $U_{\text{iso}}(\text{H}) = 1.2U_{\text{iso}}(\text{C})$ for CH and CH_2; $U_{\text{iso}}(\text{H}) = 1.5U_{\text{iso}}(\text{C or O})$ for CH_3 and OH. Appropriate restraints were applied to the geometry and thermal displacement parameters of the atoms involved in the disordered parts of the structures. The absolute configuration of cycHCs was known from synthesis, but was confirmed based on the anomalous dispersion effects. The figures were drawn using the programs Mercury CSD 3.10 [20] and POV-Ray 3.7.[21] The crystallographic data is deposited with the Cambridge Crystallographic Data Centre (CCDC 1949778-1949779) and can be obtained free of charge via www.ccdc.cam.ac.uk/data_request/cif.

Crystallographic details for the [(*R*,*R*)-cycHC[6] · ZnTPP] complex

CCDC 1949778: $C_{185}H_{206}N_{32}O_{14}Zn_2$, $M = 3232.55$ g/mol, triclinic, space group $P1$ (no. 1), $a = 12.8590(3)$ Å, $b = 13.8291(4)$ Å, $c = 24.3771(6)$ Å, $\alpha = 85.237(2)°$, $\beta = 77.006(2)°$, $\gamma = 85.321(2)°$, $V = 4200.51(19)$ Å^3, $Z = 1$, $T = 123.0$ K, $\mu(\text{CuK}\alpha) = 0.932$ mm^{-1}, $D_{calc} = 1.278$ g/cm^3, 45280 reflections measured ($3.728° \leq 2\Theta \leq 134.688°$), of which 23390 unique (19174 with $I > 2\sigma(I)$), $R_{\text{int}} = 0.0765$, $R_1[F^2 > 2\sigma(F^2)] = 0.0600$ and wR_2 (all data) = 0.1562, $S = 1.02$, Flack $x = -0.05(2)$; absolute configuration determined by anomalous diffraction effects using 5215 quotients $[(I^+)-(I^-)]/[(I^+)+(I^-)]$.

Light pink single crystals of **[(*R*,*R*)-cycHC[6] · ZnTPP] · 0.5CH$_3$OH · 0.5H$_2$O** were obtained from a solution of **(*R*,*R*)-cycHC[6]** in 1:1 tetrachloromethane and wet methanol, with 2-fold excess of **ZnTPP**. The structure crystallized in the triclinic space group $P1$, as colinear coordination polymers in the [1 1 1] direction, with a repeating unit of **[(*R*,*R*)-cycHC[6] · ZnTPP]$_n$**. The asymmetric unit contains two of the repeating units, along with solvent molecules H_2O and CH_3OH. The remaining voids in the structure (up to 35 Å^3), including those located in the cavities of **(*R*,*R*)-cycHC[6]** macrocycles, contain no significant electron density – confirmed by running the SQUEEZE algorithm of PLATON.[22] Only up to three electrons per void were found with the void search, and therefore the data deposited does not include the SQUEEZE model. Three phenyl groups were found to be disordered in the crystal structure. The relative occupancy of the respective disorder components was allowed to refine freely and is indicated on Figure S36.

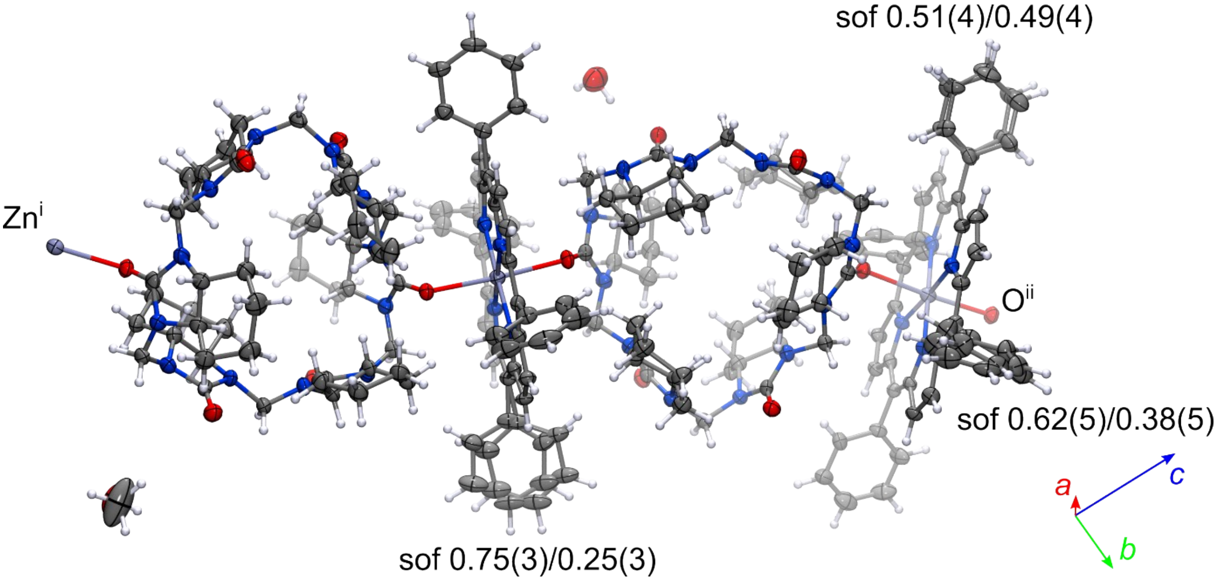

Figure S37. The asymmetric unit **2[(*R*,*R*)-cycHC[6] · ZnTPP] · CH_3OH · H_2O**, showing all the non-hydrogen atoms with the anisotropic displacement ellipsoids at 50% probability level. The site occupancy factors (sof) are indicated near the respective disorder model. The symmetry codes: i) 1+x, −1+y, −1+z; ii) −1+x, 1+y, 1+z.

Crystallographic details for the [(*R*,*R*)-cycHC[8] · 2ZnTPP] complex

CCDC 1949779: $C_{154.67}H_{158.67}Cl_4N_{24}O_{8.67}Zn_2$, M = 2764.92 g/mol, triclinic, space group $P1$ (no. 1), a = 17.6254(2) Å, b = 18.1150(2) Å, c = 35.0077(4) Å, α = 86.0710(10)°, β = 82.8330(10)°, γ = 87.1950(10)°, V = 11054.8(2) Å^3, Z = 3, T = 123.0 K, μ(CuKα) = 1.583 mm^{-1}, D_{calc} = 1.246 g/cm^3, 104000 reflections measured ($4.894° \leq 2\Theta \leq 134.974°$), of which 60400 unique (19174 with $I > 2\sigma(I)$), R_{int} = 0.0422, $R_1[F^2 > 2\sigma(F^2)]$ = 0.0625, wR_2 (all data) = 0.1927, S = 0.83. The absolute configuration of (*R*,*R*)-cycHC[8] was known from synthesis, but was confirmed based on the anomalous dispersion effects, Flack x = 0.040(11).

Single crystals of **[(*R*,*R*)-cycHC[8] · 2ZnTPP] · *n*CH_2Cl_2 · *m*CH_3OH** were obtained from a solution of **(*R*,*R*)-cycHC[8]** in a 1:1 mixture of dichloromethane and methanol in the presence of 2-fold excess of **ZnTPP**, by slow evaporation of the solvent system. Red needle-like crystals were found to be of a 1:2 complex of **(*R*,*R*)-cycHC[8]** with **ZnTPP**. The structure crystallized in the triclinic space group $P1$, with three **[(*R*,*R*)-cycHC[8] · 2ZnTPP]** moieties in the unit cell, along with solvent (CH_2Cl_2, CH_3OH) molecules. The position of seven dichloromethane molecules could be determined from the Fourier difference map. Out of these, three CH_2Cl_2 were found to be disordered. One could be modelled with two disorder components, with the relative occupancies refined freely. Two CH_2Cl_2 were modelled simply with reduced occupancy (sof 0.5), as the minor disorder components of each site could not be modelled reliably based on the Fourier difference map. Attempts to resolve the disorder of further solvent molecules failed, and therefore their contribution to the model was accounted for using the SQUEEZE method of PLATON.[22] The void analysis results and interpretation are included at the end of the CIF file. All together three cyclohexano groups of the macrocycles and one phenyl group of the porphyrin were found to be disordered in the asymmetric unit. These could be modelled with two disorder components each, with the relative occupancies refined freely.

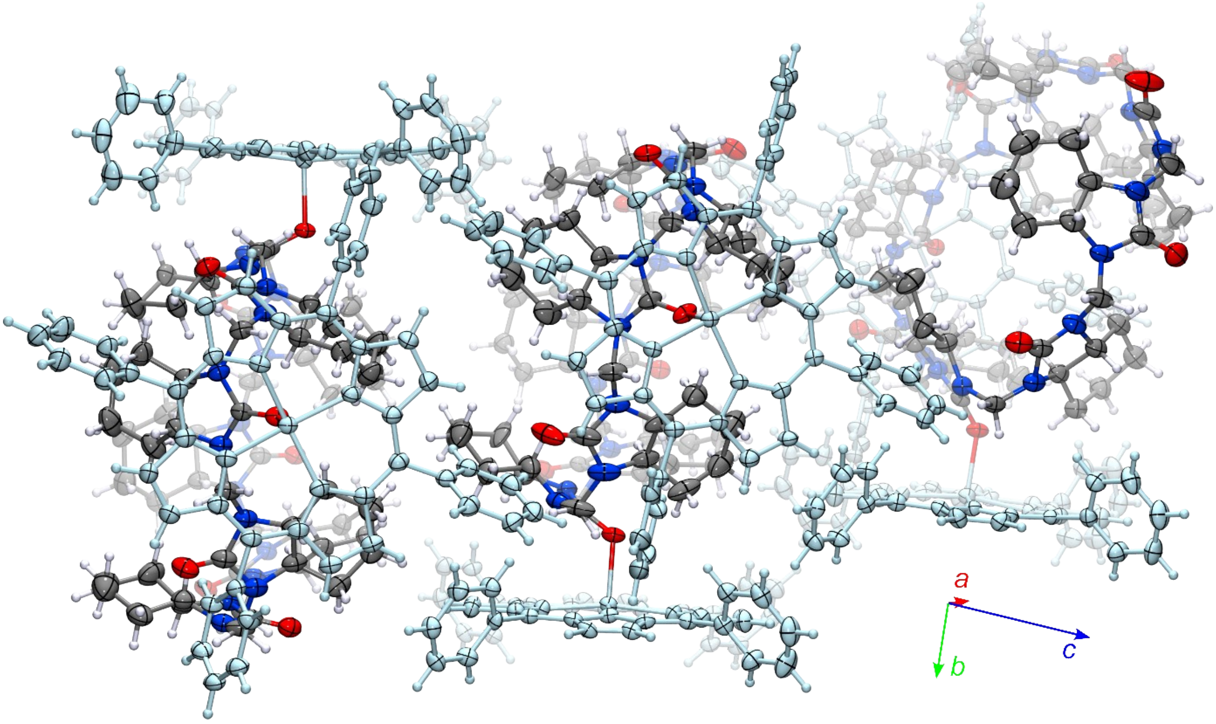

Figure S38. The asymmetric unit **3[(*R*,*R*)-cycHC[8] · 2ZnTPP]**, showing all the non-hydrogen atoms with the anisotropic displacement ellipsoids at 50% probability level. The **ZnTPP** units are coloured light blue, to improve the clarity of the figure. To this end, all solvent molecules and minor disorder components are also omitted from the figure.

Additional packing diagrams of the crystal structures

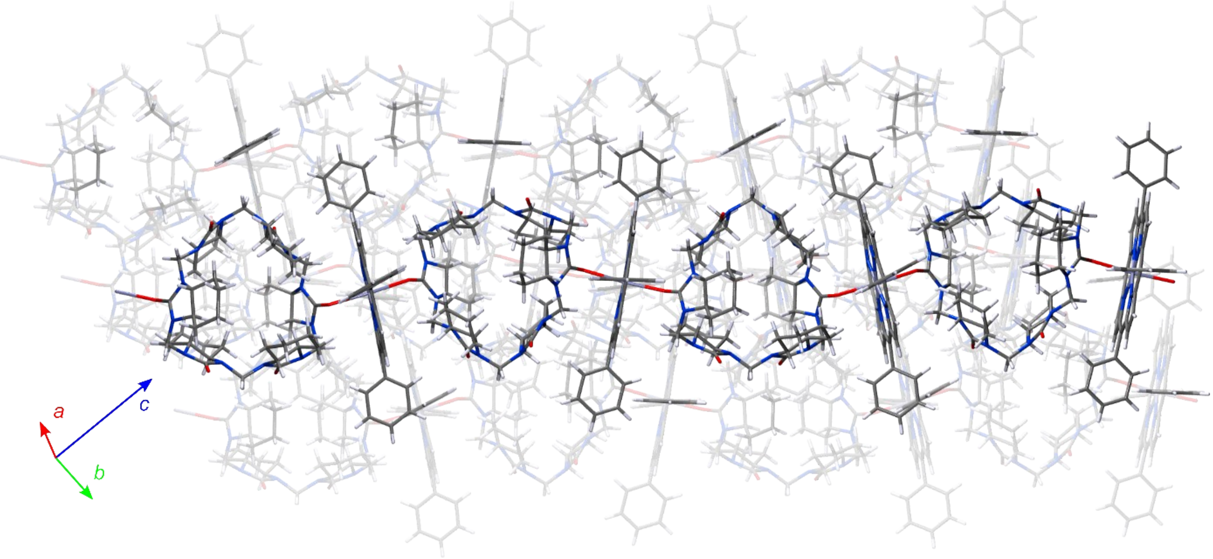

Figure S39. Side view on the packing of the 1-D coordination polymers of **[(*R*,*R*)-cycHC[6] · ZnTPP]*n***.

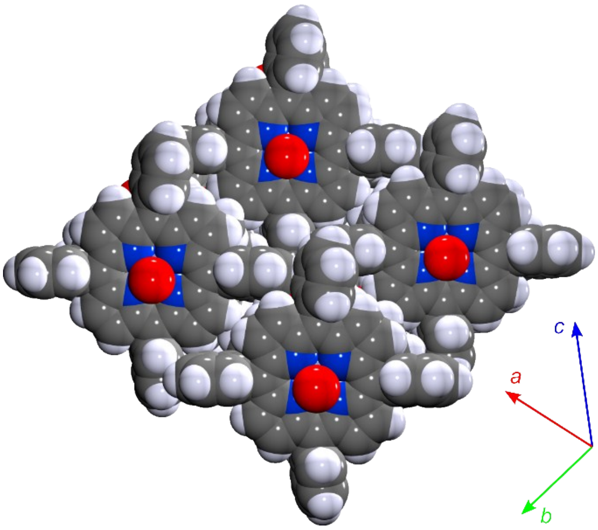

Figure S40. View along the 1-D coordination polymers of **[(*R*,*R*)-cycHC[6] · ZnTPP]*n***, drawn with the CPK atom model. The radius of the spheres corresponds to the van der Waals radii of the atom.

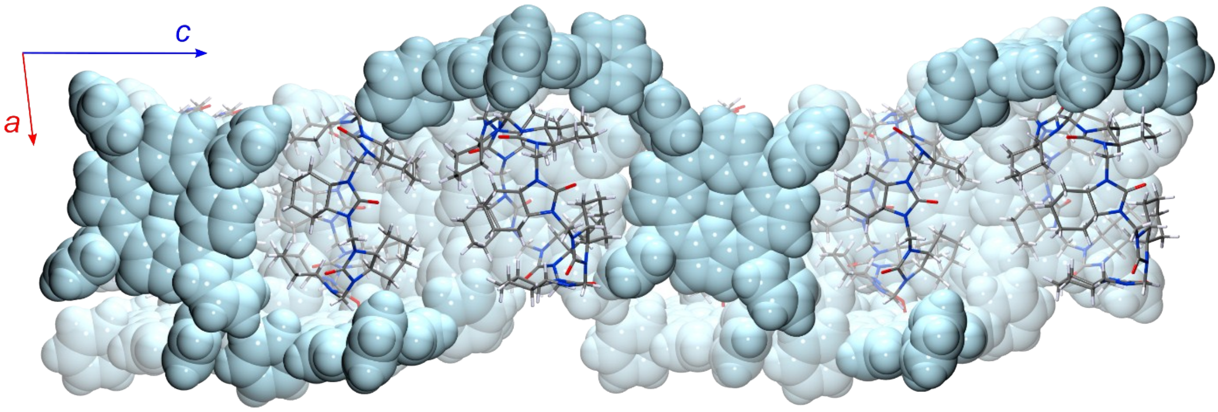

Figure S41. The packing of **[(*R*,*R*)-cycHC[8] · 2ZnTPP]**, forming channels colinear to the crystallographic *b*-axis. The **ZnTPP** units are coloured in light blue CPK model, where the radius of the spheres corresponds to the van der Waals radii of the atoms.

7. Synthesis of (*R*,*R*)-*N*,*N′*-diphenylcyclohexa-1,2-diylurea (M2)

Synthesis of new compound monourea **M2** was based on the procedure for cyclic ureas published by Lee et al.[7]

To a flask were charged (*R*,*R*)-*N*,*N′*-cyclohexa-1,2-diylurea (201 mg, 1.43 mmol), K_2CO_3 (416 mg, 3.0 mmol), CuI (27 mg, 10 mol%), (*R,R*)-*N*,*N′*-dimethylcyclohexane-1,2-diamine (40 mg, 20 mol%), bromobenzene (330 µl, 3.14 mmol ≈ 2.2 equiv) and toluene (1.8 ml) under argon. The mixture was refluxed for 20 h (while heating overnight the solvent evaporated) and then cooled to r.t., diluted with $CHCl_3$ (12 ml), and filtered through Celite and washed with $CHCl_3$ (3 × 20 ml). The organic filtrate was washed with water (3 × 20 ml), dried (anhyd. $MgSO_4$) and the solvent was completely evaporated on rotavap. Methanol (30 ml) was added to the flask and evaporated on rotavap to remove last traces of toluene. Crude product was purified by flash chromatography on silica gel, gradient elution with 0-3 % of methanol in DCM. Collected fractions were evaporated dryed under high vacuum. White solid (*R*,*R*)-*N*,*N′*-diphenylcyclohexa-1,2-diylurea was obtained (311 mg, 75 % yield). Product purity 100% according to the quantitative NMR.

Melting point: 160-163 °C

MS: $C_{19}H_{20}N_2O$, *m/z* calculated for $[M+H]^+$ 293.16 Da, found *m/z* 293.1 Da

IR (KBr, cm^{-1}): 3038 w, 2943 w, 2864 w, 1709 (CO) s, 1701 (CO) s, 1597 w, 1497 m, 1454 w, 1398 m, 1366 s, 1323 w, 1313 w, 1275 m, 1205 w, 1161 m, 1105 w, 771 m, 750 m, 712 w, 696 w, 608 w, 505 w.

^1H NMR (400 MHz, $CDCl_3$) δ (ppm) = 7.42-7.37 (m, 4H); 7.31-7.28 (m, 4H); 7.21-7.17 (m, 2H); 3.63-3.61 (m, 2H); 2.31-2.28 (m, 2H); 1.96-1.94 (m, 2H); 1.57-1.47 (m, 4H).

^{13}C NMR (101 MHz, $CDCl_3$) δ (ppm) = 159.3, 138.7, 128.8, 125.1, 123.5, 62.2, 28.5, 24.5

Optical rotation $[\alpha]_D^{25}$ = -98.5° (c = 0.406 g/dl, $CHCl_3$)

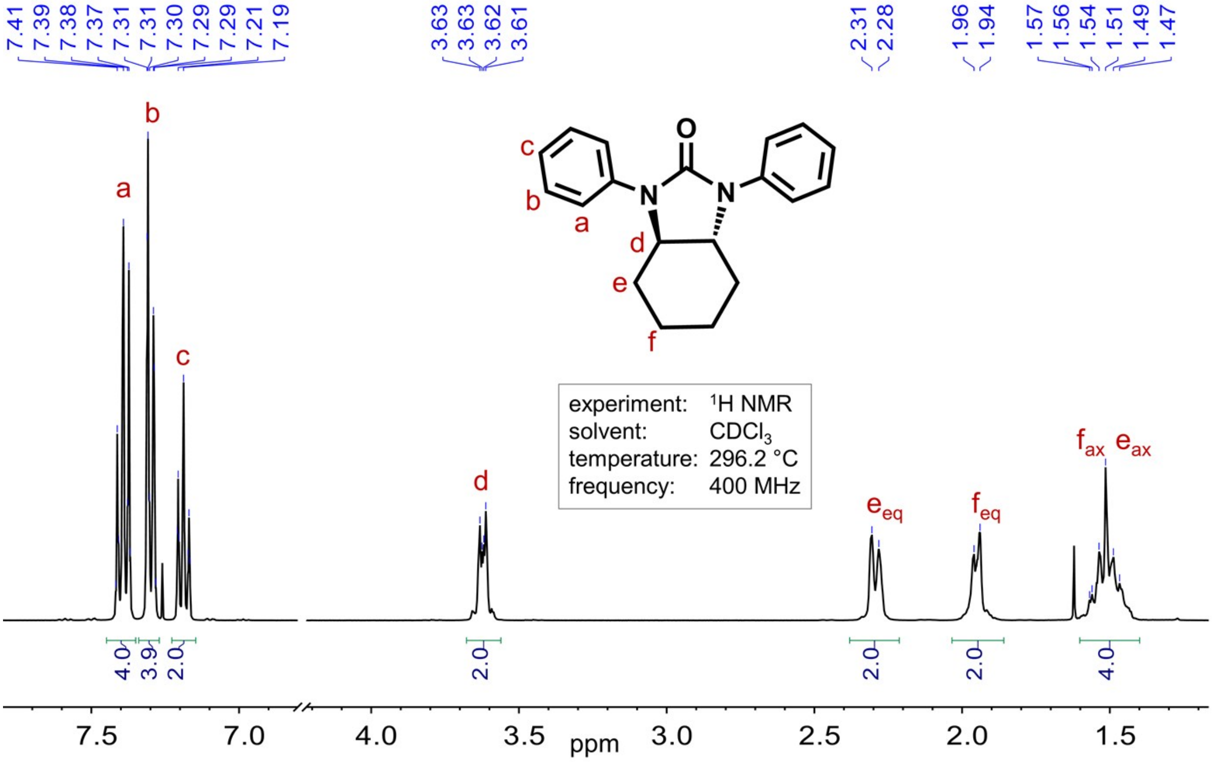
7.41
7.39
7.38
7.37
7.31
7.31
7.30
7.29
7.29
7.21
7.19
3.63
3.63
3.62
3.61
2.31
2.28
1.96
1.94
1.57
1.56
1.54
1.51
1.49
1.47
a
b
c
d
e_{eq}
f_{eq}
f_{ax} e_{ax}
O
N
N
experiment: ^{1}H NMR
solvent: $CDCl_3$
temperature: 296.2 °C
frequency: 400 MHz
4.0
3.9
2.0
2.0
2.0
2.0
4.0
7.5
7.0
4.0
3.5
ppm
3.0
2.5
2.0
1.5

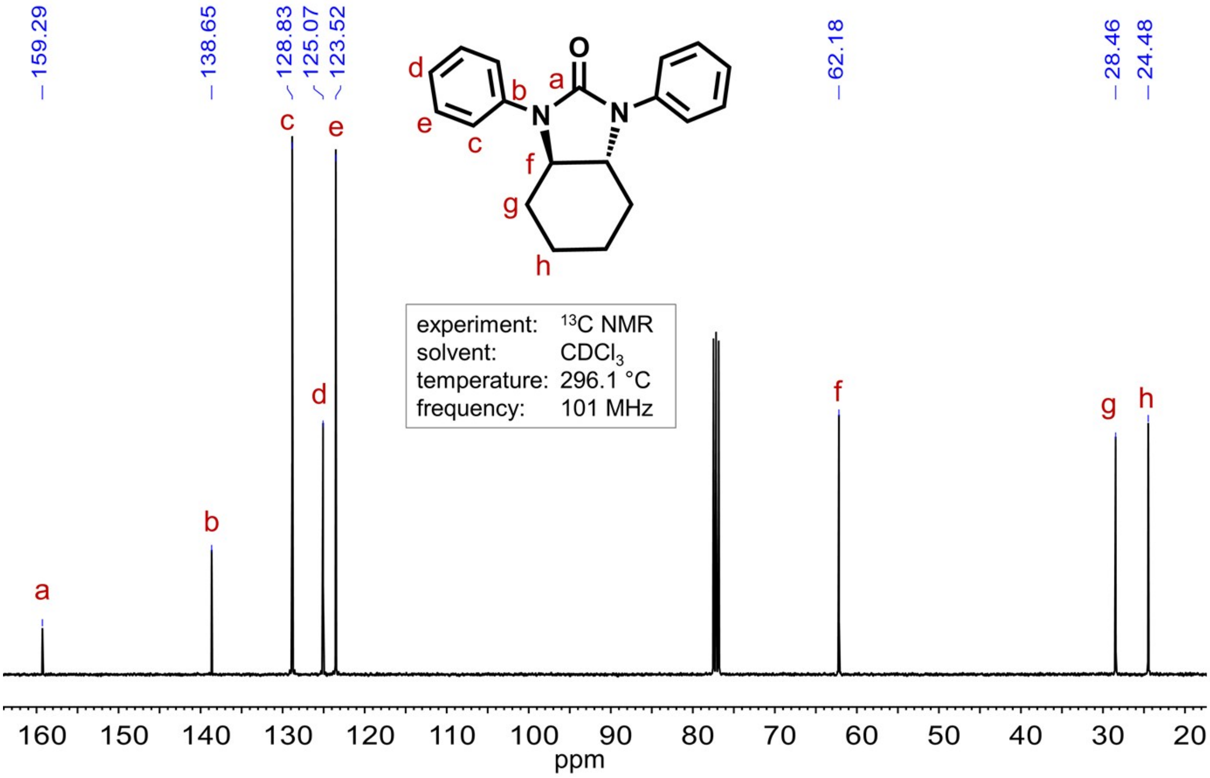
159.29
138.65
128.83
125.07
123.52
62.18
28.46
24.48
a
b
c
d
e
f
g
h
O
N
N
experiment: ^{13}C NMR
solvent: $CDCl_3$
temperature: 296.1 °C
frequency: 101 MHz
160
150
140
130
120
110
100
90
80
70
60
50
40
30
20
ppm

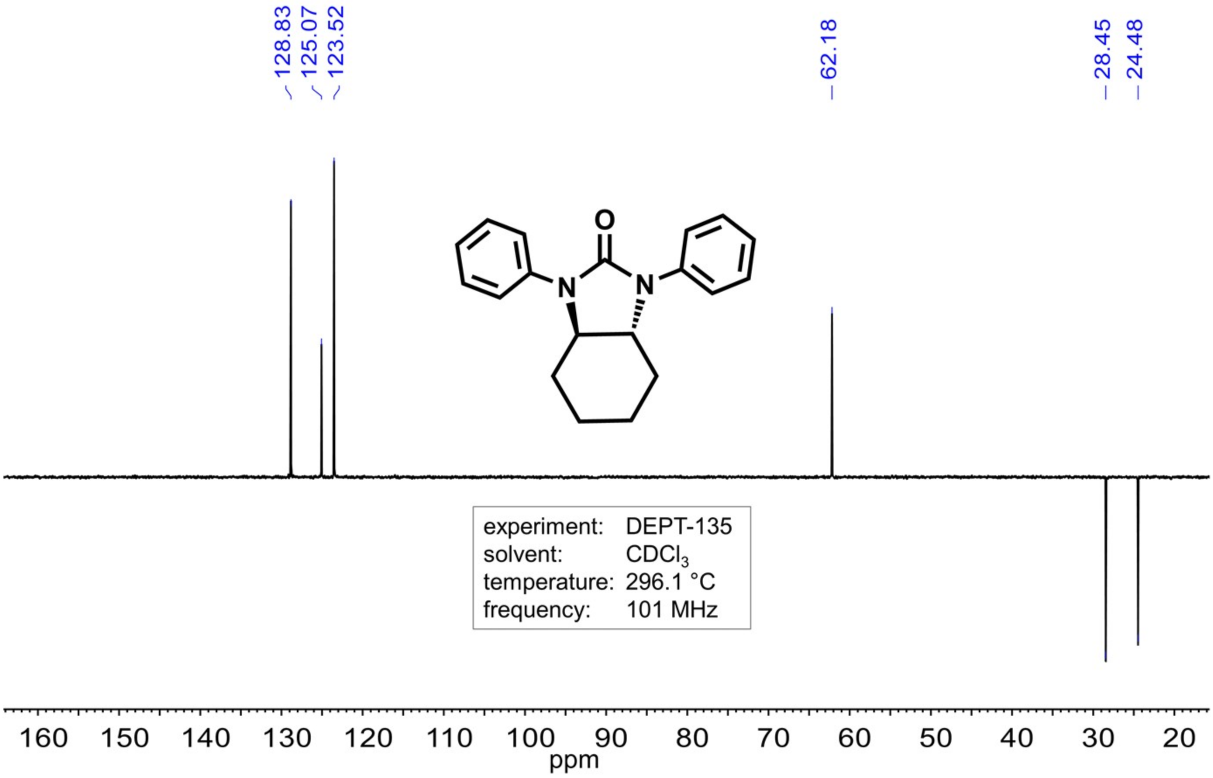
128.83
125.07
123.52
62.18
28.45
24.48
O
N
N
experiment: DEPT-135
solvent: $CDCl_3$
temperature: 296.1 °C
frequency: 101 MHz
160 150 140 130 120 110 100 90 80 70 60 50 40 30 20
ppm

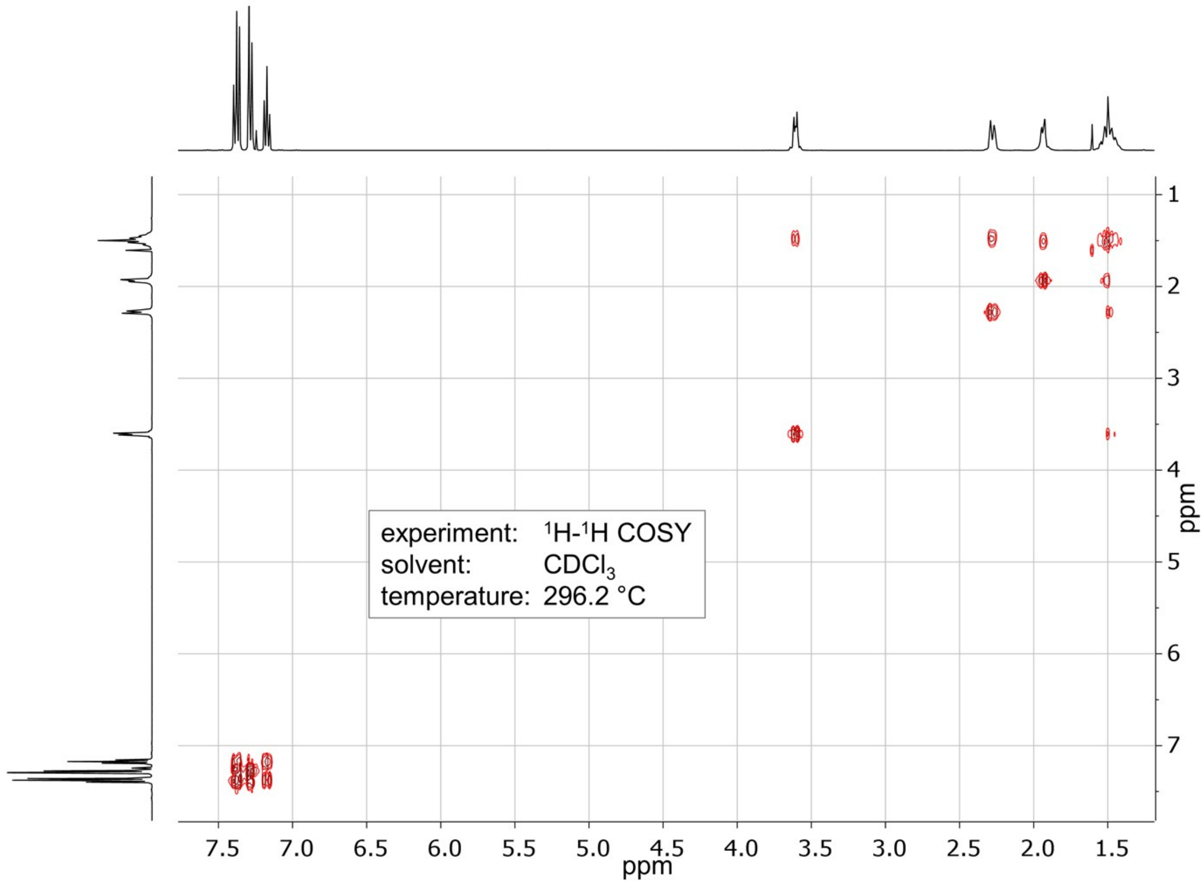
experiment: ${}^1H$-${}^1H$ COSY
solvent: $CDCl_3$
temperature: 296.2 °C
7.5 7.0 6.5 6.0 5.5 5.0 4.5 4.0 3.5 3.0 2.5 2.0 1.5
ppm
1 2 3 4 5 6 7
ppm

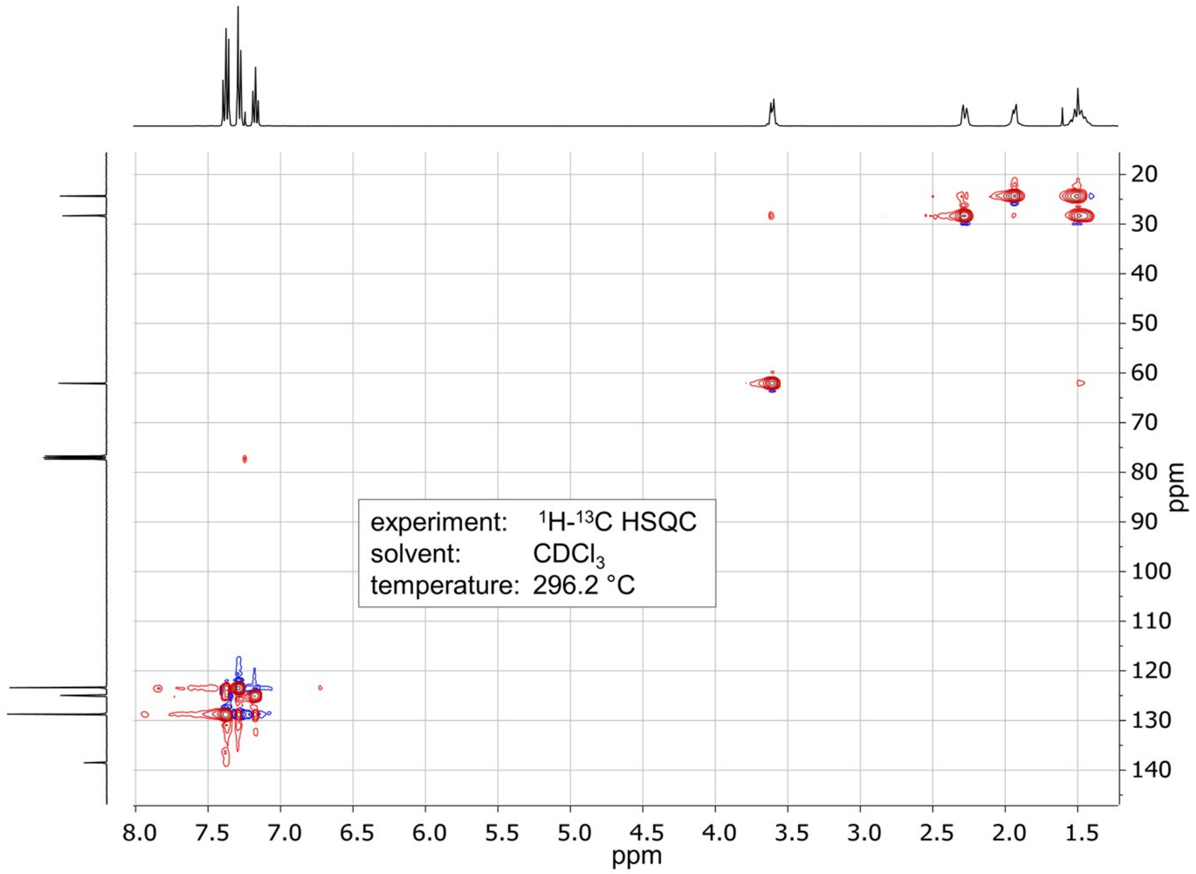
experiment: ¹H-¹³C HSQC
solvent: CDCl₃
temperature: 296.2 °C
8.0 7.5 7.0 6.5 6.0 5.5 5.0 4.5 4.0 3.5 3.0 2.5 2.0 1.5
ppm
20 30 40 50 60 70 80 90 100 110 120 130 140
ppm

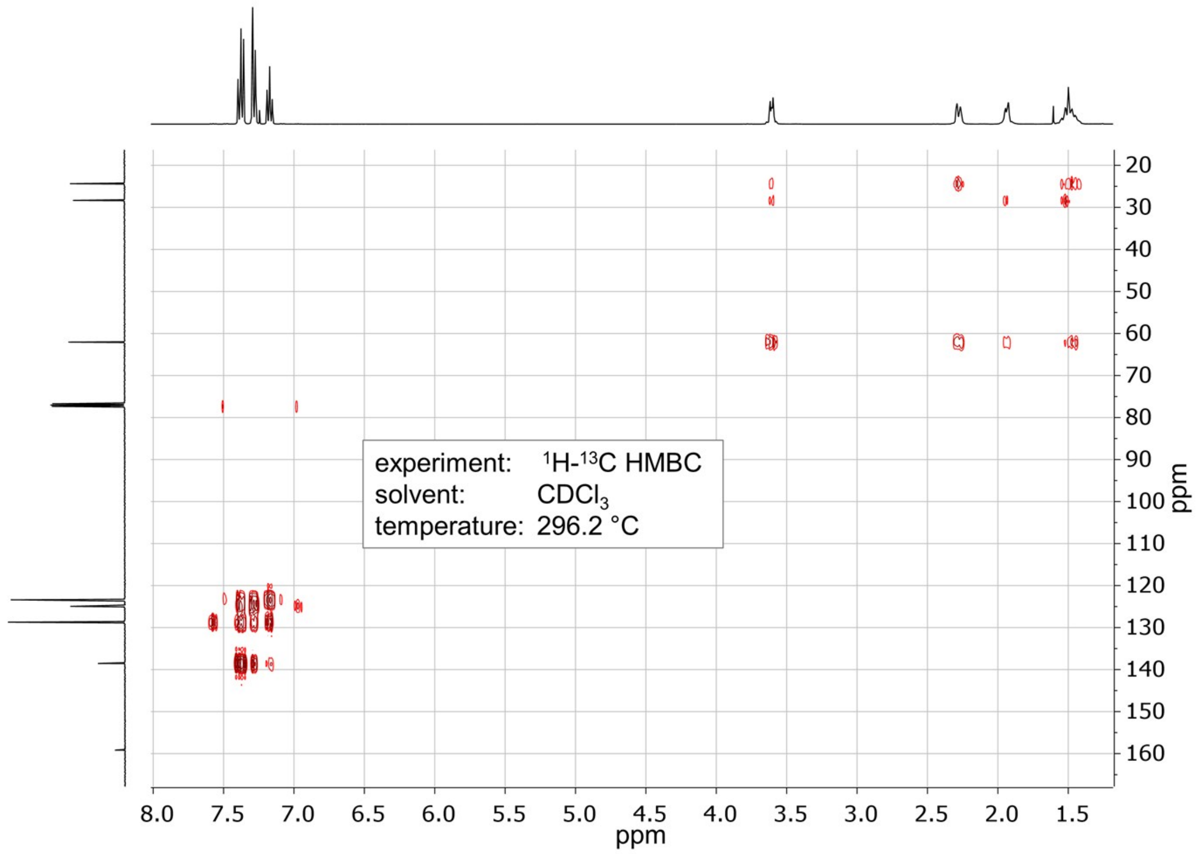
experiment: ¹H-¹³C HMBC
solvent: CDCl₃
temperature: 296.2 °C
8.0 7.5 7.0 6.5 6.0 5.5 5.0 4.5 4.0 3.5 3.0 2.5 2.0 1.5
ppm
20 30 40 50 60 70 80 90 100 110 120 130 140 150 160
ppm

8. References

1 B. C. Milgram, K. Eskildsen, S. M. Richter, W. R. Scheidt and K. A. Scheidt, *J. Org. Chem.*, 2007, **72**, 3941–3944.

2 V. V. Borovkov, J. M. Lintuluoto and Y. Inoue, *Helv. Chim. Acta*, 1999, **82**, 919–934.

3 E. Prigorchenko, M. Öeren, S. Kaabel, M. Fomitšenko, I. Reile, I. Järving, T. Tamm, F. Topić, K. Rissanen and R. Aav, *Chem. Commun.*, 2015, **51**, 10921–10924.

4 R. Aav, E. Shmatova, I. Reile, M. Borissova, F. Topić and K. Rissanen, *Org. Lett.*, 2013, **15**, 3786–3789.

5 C.-D. Li, S. L. Mella and A. C. Sartorelli, *J. Med. Chem.*, 1981, **24**, 1089–1092.

6 E. Prigorchenko, S. Kaabel, T. Narva, A. Baškir, M. Fomitšenko, J. Adamson, I. Järving, K. Rissanen, T. Tamm and R. Aav, *Chem. Commun.*, 2019, **55**, 9307–9310.

7 C.-C. Lee, P.-S. Wang, M. B. Viswanath and M. Leung, *Synthesis*, 2008, **2008**, 1359–1366.

8 M. J. Frisch, G. W. Trucks, H. B. Schlegel, G. E. Scuseria, M. A. Robb, J. R. Cheeseman, G. Scalmani, V. Barone, G. A. Petersson, H. Nakatsuji, X. Li, M. Caricato, A. V. Marenich, J. Bloino, B. G. Janesko, R. Gomperts, B. Mennucci, H. P. Hratchian, J. V. Ortiz, A. F. Izmaylov, J. L. Sonnenberg, Williams, F. Ding, F. Lipparini, F. Egidi, J. Goings, B. Peng, A. Petrone, T. Henderson, D. Ranasinghe, V. G. Zakrzewski, J. Gao, N. Rega, G. Zheng, W. Liang, M. Hada, M. Ehara, K. Toyota, R. Fukuda, J. Hasegawa, M. Ishida, T. Nakajima, Y. Honda, O. Kitao, H. Nakai, T. Vreven, K. Throssell, J. A. Montgomery Jr., J. E. Peralta, F. Ogliaro, M. J. Bearpark, J. J. Heyd, E. N. Brothers, K. N. Kudin, V. N. Staroverov, T. A. Keith, R. Kobayashi, J. Normand, K. Raghavachari, A. P. Rendell, J. C. Burant, S. S. Iyengar, J. Tomasi, M. Cossi, J. M. Millam, M. Klene, C. Adamo, R. Cammi, J. W. Ochterski, R. L. Martin, K. Morokuma, O. Farkas, J. B. Foresman and D. J. Fox, *Gaussian 16 Rev. A.01*, Wallingford, CT, 2016.

9 J. P. Perdew, K. Burke and M. Ernzerhof, *Phys. Rev. Lett.*, 1996, **77**, 3865–3868.

10 J. P. Perdew, K. Burke and M. Ernzerhof, *Phys. Rev. Lett.*, 1997, **78**, 1396–1396.

11 F. Weigend and R. Ahlrichs, *Phys. Chem. Chem. Phys.*, 2005, **7**, 3297–3305.

12 F. Weigend, *Phys. Chem. Chem. Phys.*, 2006, **8**, 1057–1065.

13 T. Yanai, D. P. Tew and N. C. Handy, *Chem. Phys. Lett.*, 2004, **393**, 51–57.

14 W. Minor, M. Cymborowski, Z. Otwinowski and M. Chruszcz, *Acta Crystallogr. D Biol. Crystallogr.*, 2006, **62**, 859–866.

15 *CrysAlisPRO*, Agilent Technologies Ltd, 2014.

16 R. C. Clark and J. S. Reid, *Acta Crystallogr. A*, 1995, **51**, 887–897.

17 G. M. Sheldrick, *Acta Crystallogr. Sect. Found. Adv.*, 2015, **71**, 3–8.

18 G. M. Sheldrick, *Acta Crystallogr. Sect. C Struct. Chem.*, 2015, **71**, 3–8.

19 O. V. Dolomanov, L. J. Bourhis, R. J. Gildea, J. a. K. Howard and H. Puschmann, *J. Appl. Crystallogr.*, 2009, **42**, 339–341.

20 C. F. Macrae, P. R. Edgington, P. McCabe, E. Pidcock, G. P. Shields, R. Taylor, M. Towler and J. van de Streek, *J. Appl. Crystallogr.*, 2006, **39**, 453–457.

21 *Persistence of Vision Raytracer*, Persistence of Vision Pty. Ltd., 2004.

22 A. L. Spek, *Acta Crystallogr. D Biol. Crystallogr.*, 2009, **65**, 148–155.